Traveling-Wave Tubes

By J. R. PIERCE

[FOURTH INSTALLMENT]

CHAPTER XII

POWER OUTPUT

A THEORETICAL EVALUATION of the power output of a traveling-wave tube requires a theory of the non-linear behavior of the tube. In this book we have dealt with a linearized theory only. No attempt will be made to develop a non-linear theory. Some results of non-linear theory will be quoted, and some conclusions drawn from experimental work will be presented.

One thing appears clear both from theory and from experiment: the gain parameter C is very important in determining efficiency. This is perhaps demonstrated most clearly in some unpublished work of A. T. Nordsieck.

Nordsieck assumed:

(1) The same a-c field acts on all electrons.
(2) The only fields present are those associated with the circuit ("neglect of space charge").
(3) Field components of harmonic frequency are neglected.
(4) Backward-traveling energy in the circuit is neglected.
(5) A lossless circuit is assumed.
(6) C is small (it always is).

Nordsieck obtained numerical solutions for such cases for several electron velocities. He found the maximum efficiency to be proportonal to C by a factor we may call k. Thus, the power output P is

$$P = kCI_0V_0 \tag{12.1}$$

In Fig. 12.1, the factor k is plotted vs. the velocity parameter b. For an electron velocity equal to that of the unperturbed wave the fractional efficiency obtained is $3C$; for a faster electron velocity the efficiency rises to $7C$. For instance, if $C = .025$, $3C$ is 7.5% and $7C$ is 15%. For 1,600 volts 15 ma this means 1.8 or 3.6 watts. If, however, $C = 0.1$, which is attainable, the indicated efficiency is 30% to 70%.

Experimental efficiencies often fall very far below such figures, although some efficiencies which have been attained lie in this range. There are three apparent reasons for these lower efficiencies. First, small non-uniformities in wave propagation set up new wave components which abstract energy from the increasing wave, and which may subtract from the normal output. Second, when the a-c field varies across the electron flow, not all electrons

are acted on equally favorably. Third, most tubes have a central lossy section followed by a relatively short output section. Such tubes may overload so severely in the lossy section that a high level in the output section is never attained. There is not enough length of loss-free circuit to provide sufficient gain in the output circuit so that the signal can build up to maximum amplitude from a low level increasing wave. Other tubes with distributed loss suffer because the loss cuts down the efficiency.

Some power-series non-linear calculations made by L. R. Walker show that for fast velocities of injection the first non-linear effect should be an expansion, not a compression. Nordsieck's numerical solutions agree with this. A power series approach is inadequate in dealing with truly large-signal be-

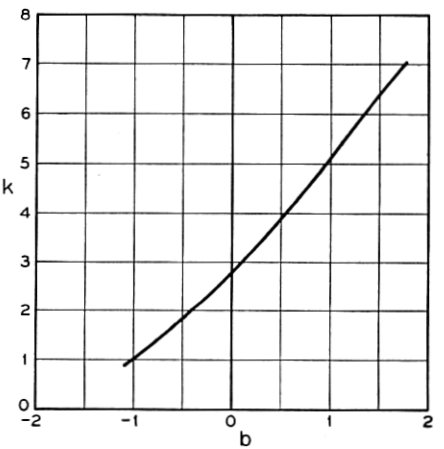

Fig. 12.1—The calculated efficiency is expressed as kC, where k is a function of the velocity parameter b. This curve shows k as given by Nordsieck's high-level calculations.

havior. In fact, Nordsieck's work shows that the power-series attack, if based on an assumption that there is no overtaking of electrons by electrons emitted later, must fail at levels much below the maximum output.

Further work by Nordsieck indicates that the output may be appreciably reduced by variation of the a-c field across the beam.

It is unfortunate that Nordsieck's calculations do not cover a wider range of conditions. Fortunately, unlikely as it might seem, the linear theory can tell us a little about what limitation of power we might expect. For instance, from (7.15) we have

$$\frac{v}{u_0} = -j\frac{\eta V}{u_0^2 \delta C}$$

$$\frac{v}{u_0} = -j\left(\frac{V}{2V_0}\right)\left(\frac{1}{\delta C}\right) \tag{12.2}$$

while from (7.16) we have

$$\frac{i}{I_0} = -\left(\frac{V}{2V_0}\right)\left(\frac{1}{\delta C}\right)^2 \tag{12.3}$$

We expect non-linear effects to become important when an a-c quantity is no longer small compared with a d-c quantity. We see that because $(1/\delta C)$ is large, $|\, i/I_0 \,|$ will be larger than $|\, v/u_0 \,|$.

The important non-linearity is a sort of over-bunching or limit to bunching. For instance, suppose we were successful in bunching the electron flow into very short pulses of electrons, as shown in Fig. 12.2 As the pulses approach zero length, the ratio of the peak value of the fundamental component of convection current to the average or d-c current I_0 approaches 2. We may, then, get some hint as to the variation of power output as various parameters are varied by letting $|\, i \,| = 2I_0$ and finding the variation of power in the circuit for an a-c convection current as we vary various parameters.

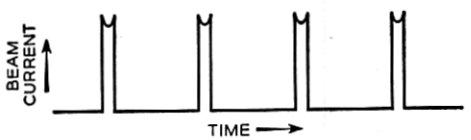

Fig. 12.2—If the electron beam were bunched into pulses short compared with a cycle, the peak value of the component of fundamental frequency would be twice the d-c current I_0.

Deductions made in this way cannot be more than educated guesses, but in the absence of non-linear calculations they are all we have.

From (7.1) we have for the *circuit field* associated with the *active mode* (neglecting the field due to space charge)

$$E = \frac{\Gamma^2 \Gamma_1 (E^2/\beta^2 P)}{2(\Gamma_1^2 - \Gamma^2)} \tag{12.4}$$

This relation is, of course, valid only for an electron convection current i which varies with distance as $\exp(-\Gamma z)$. For the power to be large for a given magnitude of current, E should be large. For a given value of i, E will be large if Γ is very nearly equal to Γ_1. This is natural. If Γ were equal to Γ_1, the natural propagation constant of the circuit, the contribution to the field by the current i in every elementary distance would have such phase as to add in phase with every other contribution.

Actually, Γ_1 and Γ cannot be quite equal. We have from (7.10) and (7.11)

$$-\Gamma_1 = \beta_e(-j - jCb - Cd) \tag{12.5}$$

$$-\Gamma = \beta_e(-j + jCy_1 + Cx_1) \tag{12.6}$$

For a physical circuit the attenuation parameter d must be positive while, for an increasing wave, x must be positive. We see that we may expect E to be greatest for a given current when d and x are small, and when y is nearly equal to the velocity parameter b.

Suppose we use (12.4) in expressing the power

$$P = \frac{E^2}{\beta^2(E^2/\beta^2 P)} = \left| \frac{\Gamma^4 \Gamma_1^2 (E^2/\beta^2 P)}{4\beta^2(\Gamma_1^2 - \Gamma^2)^2} i^2 \right|. \tag{12.7}$$

Here we identify β with $-j\Gamma_1$. Further, we use (2.43), (12.5) and (12.6), and assuming C to be small, neglect terms involving C compared with unity. We will further let i have a value

$$i = 2I_0 \tag{12.8}$$

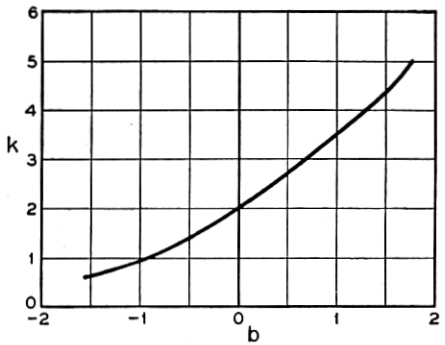

Fig. 12.3—An efficiency parameter k calculated by taking the power as that given by near theory for an r-f beam current with a peak value twice the d-c beam current.

We obtain

$$P = kCI_0V_0 \tag{12.9}$$

$$k = \frac{2}{(b + y)^2 + (x + d)^2} \tag{12.10}$$

We will now investigate several cases. Let us consider first the case of a lossless circuit ($d = 0$) and no space charge ($QC = 0$) and plot the efficiency factor k vs. b. The values of x and y are those of Fig. 8.1. Such a plot is shown in Fig. 12.3.

If we compare the curve of Fig. 12.3 with the correct curve of Nordsieck, we see that there is a striking qualitative agreement and, indeed, fair quantitative agreement. We might have expected on the one hand that the electron stream would never become completely bunched ($i = 2I_0$) and that, as it approached complete bunching, behavior would already be non-linear. This would tend to make (12.10) optimistic. On the other hand, even after i

attains its maximum value and starts to fall, power can still be transferred to the circuit, though the increase of field with distance will no longer be exponential. This makes it possible that the value of k given by (12.10) will be exceeded. Actually, the true k calculated by Nordsieck is a little higher than that given by (12.10).

Let us now consider the effect of loss. Figure 12.4 shows k from (12.10) vs. d for $b = QC = 0$. We see that, as might be expected, the efficiency falls as the loss is increased. C. C. Cutler has shown experimentally through unpublished work that the power actually falls off much more rapidly with d.

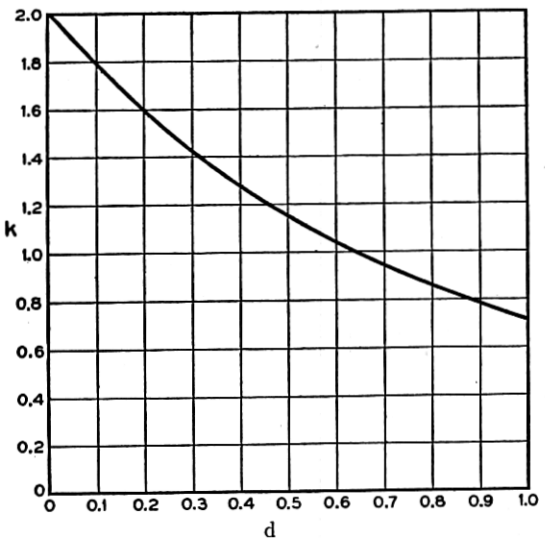

Fig. 12.4—The efficiency parameter k calculated as in Fig. 12.3 but for $b = 0$ (an electron velocity equal to the circuit phase velocity) and for various values of the attenuation parameter d. Experimentally, the efficiency falls off more rapidly as d is increased.

Finally, Fig. 12.5 shows k from (12.10) vs. QC, with $d = 0$ and b chosen to make x_1 a maximum. We see that there is a pronounced rise in efficiency as the space-charge parameter QC is increased.

J. C. Slater has suggested in Microwave Electronics a way of looking at energy production essentially based on observing the motions of electrons while traveling along with the speed of the wave. He suggests that the electrons might eventually be trapped and oscillate in the troughs of the sinusoidal field. If so, and if they initially have an average velocity Δv greater than that of the wave, they cannot emerge with a velocity lower than the velocity of the wave less Δv. Such considerations are complicated by the fact that the phase velocity of the wave in the large-signal region will not

be the same as its phase velocity in the small-signal region. It is interesting, however, to see what limiting efficiencies this leads to.

The initial electron velocity for the increasing wave is approximately

$$v_a = v_c(1 - y_1 C) \tag{12.11}$$

where v_c is the phase velocity of the wave in the absence of electrons. The quantity y_1 is negative. According to Slater's reckoning, the final electron velocity cannot be less than

$$v_b = v_c(1 + y_1 C) \tag{12.12}$$

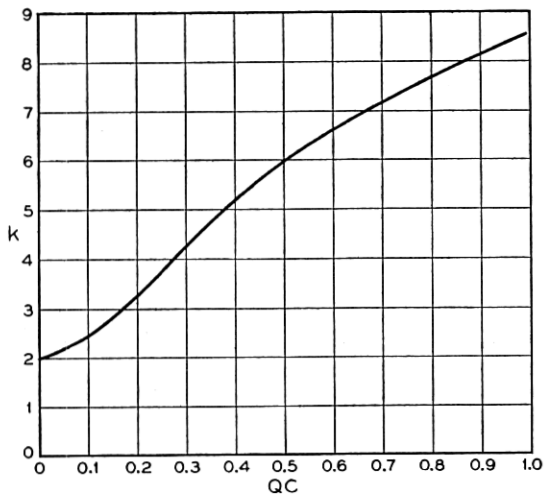

Fig. 12.5—The efficiency parameter k calculated as in Fig. 12.3, for zero loss and for an electron velocity which makes the gain of the increasing wave greatest, vs the space-charge parameter QC.

The limiting efficiency η accordingly will be, from considerations of kinetic energy

$$\eta = \frac{v_a^2 - v_b^2}{v_a^2}$$

$$\eta = \frac{4y_1 C}{(1 - y_1 C)^2}.$$

If $y_1 C \ll 1$, very nearly

$$\eta = 4\, y_1 C \tag{12.13}$$

We see that this also indicates an efficiency proportional to C. In Fig. 12.6 $4y_1$ is plotted vs. b for $QC = d = 0$. We see that this quantity ranges

from 2 for $b = 0$ up to 5 for larger values of b. It is surprising how well this agrees with corresponding values of 3 and 7 from Nordsieck's work. Moreover (12.13) predicts an increase in efficiency with increasing QC.

Thus, we may expect the efficiency to vary with C from several points of view.

It is interesting to consider what happens if at a given frequency we change the current. By changing the current while holding the voltage constant we increase both the input power and the efficiency, for C varies as $I_0^{1/3}$. Thus, in changing the current alone we would expect the power to vary as the 4/3 power of I_0

$$P \approx I_0^{4/3} \tag{12.14}$$

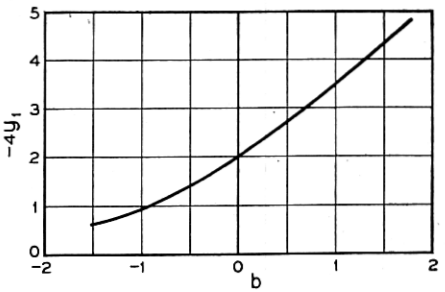

Fig. 12.6—According to a suggestion made by Slater, the velocity by which the electrons are slowed down cannot be greater than twice the difference between the electron velocity and the wave velocity. If we use the velocity difference given by the linear theory, for zero loss ($d = 0$) this would make the efficiency parameter k equal to $-4y_1$. Here $-4y_1$ is plotted vs b for $QC = 0$.

Here space charge has been neglected, and actually power may increase more rapidly with current than (12.14) indicates.

A variety of other cases can be considered. At a given voltage and current, C and the efficiency rise as the helix diameter is made smaller. However, as the helix diameter is made smaller it may be necessary to decrease the current, and the optimum gain will come at higher frequencies. For a given beam diameter, the magnetic focusing field required to overcome space-charge repulsion is constant if $I_0/V_0^{1/2}$ is held constant, and hence we might consider increasing the current as the 1/2 power of the voltage, and thus increasing the power input as the 3/2 power of the voltage. On the other hand, the magnetic focusing field required to correct initial angular deflections of electrons increases as the voltage is raised.

There is no theoretical reason why electrons should strike the circuit. Thus, it is theoretically possible to use a very high beam power in connection with a very fragile helix. Practically, an appreciable fraction of the beam current is intercepted by the helix, and this seems unavoidable for wave

lengths around a centimeter or shorter, for accurate focusing becomes more difficult as tubes are made physically smaller. Thus, in getting very high powers at ordinary wavelengths or even moderate powers at shorter wavelengths, filter type circuits which provide heat dissipation by thermal conduction may be necessary. We have seen that the impedance of such circuits is lower than that of a helix for the broadband condition (group velocity equal to phase velocity). However, high impedances and hence large values of C can be attained at the expense of bandwidth by lowering the group velocity. This tends to raise the efficiency, as do the high currents which are allowable because of good heat dissipation. However, lowering group velocity increases attenuation, and this will tend to reduce efficiency somewhat.

It has been suggested that the power can be increased by reducing the phase velocity of the circuit near the output end of the tube, so that the electrons which have lost energy do not fall behind the waves. This is a complicated but attractive possibility. It has also been suggested that the electrode which collects electrons be operated at a voltage lower than that of the helix.

The general picture of what governs and limits power output is fairly clear as long as C is very small. If attenuation near the output of the tube is kept small, and the circuit is constructed so as to approximate the requirement that nearly the same field acts on all electrons, efficiencies as large as 40% are indicated within the limitations of the present theory. With larger values of C it is not clear what the power limitation will be.

The usual traveling-wave tube would seem to have a serious competitor for power applications in the traveling-wave magnetron amplifier, which is discussed briefly in a later chapter.

CHAPTER XIII

TRANSVERSE MOTION OF ELECTRONS

Synopsis of Chapter

SO FAR WE HAVE taken into account only longitudinal motions of electrons. This is sufficient if the transverse fields are small compared to the longitudinal fields (as, near the axis of an axially symmetrical circuit) or, if a strong magnetic focusing field is used, so that transverse motions are inhibited. It is possible, however, to obtain traveling-wave gain in a tube in which the longitudinal field is zero at the mean position of the electron beam. For a slow wave, the electric field is purely transverse only along a plane. The transverse field in this plane forces electrons away from the plane and preferentially throws them into regions of retarding field, where they give up energy to the circuit. This mechanism is not dissimilar to that in the longitudinal field case, in which the electrons are moved longitudinally from their unperturbed positions, preferentially into regions of more retarding field.

Whatever may be said about tubes utilizing transverse fields, it is certainly true that they have been less worked on than longitudinal-field tubes. In view of this, we shall present only a simple analysis of their operation along the lines of Chapter II. In this analysis we take cognizance of the fact that the charge induced in the circuit by a narrow stream of electrons is a function not only of the charge per unit length of the beam, but of the distance between the beam and the circuit as well.

The factor of proportionality between distance and induced charge can be related to the field produced by the circuit. Thus, if the variation of V in the x, y plane (normal to the direction of propagation) is expressed by a function Φ, as in (13.3), the effective charge ρ_E is expressed by (13.8) and, if y is the displacement of the beam normal to the z axis, by (13.9) where Φ' is the derivative of Φ with respect to y.

The equations of motion used must include displacements normal to the z direction; they are worked out including a constant longitudinal magnetic focusing field. Finally, a combined equation (13.23) is arrived at. This is rewritten in terms of dimensionless parameters, neglecting some small terms, as (13.26)

$$j\delta - b = \frac{1}{\delta^2} + \frac{\alpha^2}{(\delta^2 + f^2)}.$$

Here δ and b have their usual meanings; α is the ratio between the transverse and longitudinal field strengths, and f is proportional to the strength of the magnetic focusing field.

In case of a purely transverse field, a new gain parameter D is defined. D is the same as C except that the longitudinal a-c field is replaced by the transverse a-c field. In terms of D, b and δ are redefined by (13.36) and (13.37), and the final equation is (13.38). Figures 13.5–13.10 show how the x's and y's vary with b for various values of f (various magnetic fields) and Fig. 13.11 shows how x_1, which is proportional to the gain of the increasing wave in db per wavelength, decreases as magnetic field is increased. A numerical example shows that, assuming reasonable circuit impedance, a magnetic field which would provide a considerable focusing action would still allow a reasonable gain.

The curves of Figs. 13.6–13.10 resemble very much the curves of Figs. 8.7–8.9 of Chapter VIII, which show the effect of space charge in terms of the parameter QC. This is not unnatural; in one case space charge forces tend to return electrons which are accelerated longitudinally to their undisturbed positions. In the other case, magnetic forces tend to return electrons which are accelerated transversely to their undisturbed positions. In each case the circuit field acts on an electron stream which can itself sustain oscillations. In one case, the oscillations are of a plasma type, and the restoring force is caused by space charge of the bunched electron stream; in the other case the electrons can oscillate transversely in the magnetic field with cyclotron frequency.

Let us, for instance, compare (7.13), which applies to purely longitudinal displacements with space charge, with (13.38), which applies to purely transverse fields with a longitudinal magnetic field. For zero loss ($d = 0$), (7.13) becomes

$$1 = (j\delta - b)(\delta^2 + 4QC)$$

While

$$1 = (j\delta - b)(\delta^2 + f^2) \tag{13.38}$$

describes the transverse case. Thus, if we let

$$4QC = f^2$$

the equations are identical.

When there is both a longitudinal and a transverse electric field, the equation for δ is of the fifth degree. Thus, there are five forward waves. For an electron velocity equal to the circuit phase velocity ($b = 0$) and for no attenuation, the two new waves are unattenuated.

If there is no magnetic field, the presence of a transverse field component merely adds to the gain of the increasing wave. If a small magnetic field is

imposed in the presence of a transverse field component, this gain is somewhat reduced.

13.1 Circuit Equation

Consider a tubular electrode connected to ground through a wire, shown in Fig. 13.1. Suppose we bring a charge Q into the tube from ∞. A charge Q will flow to ground through the wire. This is the situation assumed in the analysis of Chapter II. In Fig. 2.3 it is assumed that all the lines of force from the charge in the electron beam terminate on the circuit, so that the whole charge may be considered as impressed on the circuit.

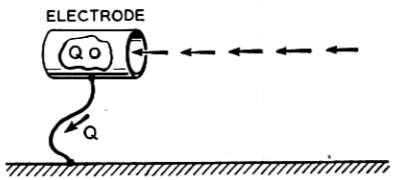

Fig. 13.1—When a charge Q approaches a grounded conductor from infinity and in the end all the lines of force from the charge end on the conductor, a charge Q flows in the grounding lead.

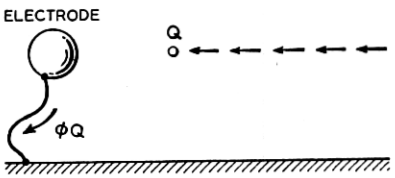

Fig. 13.2—If a charge Q approaches a conductor from infinity but in the end only part of the lines of force from the charge end on the conductor, a charge ΦQ flows in the grounding lead, where $\Phi < 1$.

Now consider another case, shown in Fig. 13.2, in which a charge Q is brought from ∞ to the vicinity of a grounded electrode. In this case, not all of the lines of force from the charge terminate on the electrode, and a charge ΦQ which is smaller than Q flows through the wire to ground.

We can represent the situation of Fig. 13.2 by the circuit shown in Fig. 13.3. Here C_2 is the capacitance between the charge and the electrode and C_1 is the capacitance between the charge and ground. We see that the charge ΦQ which flows to ground when a charge Q is brought to a is

$$\Phi Q = QC_2/(C_1 + C_2) \tag{13.1}$$

Now suppose we take the charge Q away and hold the electrode at a potential V with respect to ground, as shown in Fig. 13.4. What is the potential V_a at a? We see that it is

$$V_a = [C_2/(C_1 + C_2)]V = \Phi V \tag{13.2}$$

Thus, the same factor Φ relates the actual charge to the "effective charge" acting on the circuit and the actual circuit voltage to the voltage produced at the location of the charge.

We will not consider in this section the "space charge" voltage produced by the charge itself (the voltage at point a in Fig. 13.4).

The circuit voltage V we consider as varying as $\exp(-\Gamma z)$ in the direction of propagation. The voltage in the vicinity of the circuit is given by

$$V(x, y) = \Phi V \tag{13.3}$$

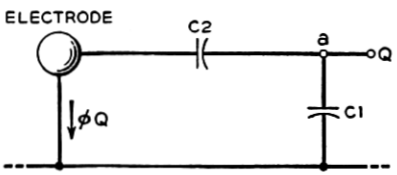

Fig. 13.3—The situation of Fig. 13.2 results in the same charge flow as if the charge were put on terminal a of the circuit shown, which consists of two capacitors of capacitances C_1 and C_2.

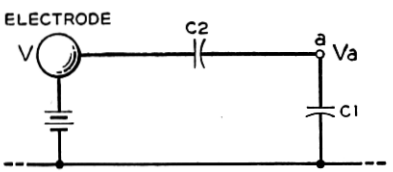

Fig. 13.4—A voltage V inserted in the ground lead divides across the condensers so that $V_a = \Phi V$, where Φ is the same factor which relates the charge flowing in the ground lead to the charge Q applied at a in Figs. 13.2 and 13.3.

Here x and y refer to coordinates normal to z and Φ is a function of x and y. We will choose x and y so

$$\partial\Phi/\partial x = 0 \tag{13.4}$$

Then

$$E_y = -V\partial\Phi/\partial y = -\Phi' V \tag{13.5}$$

$$\Phi' = \partial\Phi/\partial y \tag{13.6}$$

In (13.3), Φ will vary somewhat with Γ, but, as we are concerned with a small range only in Γ, we will consider Φ a function of y only.

From Chapter II we have

$$V = \frac{-\Gamma\Gamma_1 Ki}{(\Gamma^2 - \Gamma_1^2)} \tag{2.10}$$

and

$$\rho = \frac{-j\Gamma i}{\omega}. \tag{2.18}$$

So that

$$V = \frac{-j\omega\Gamma_1 K\rho}{(\Gamma^2 - \Gamma_1^2)}. \tag{13.7}$$

In (13.7), it is assumed that $\Phi = 1$. If $\Phi \neq 1$, we should replace ρ in (13.7) by the a-c component of effective charge. The total effective charge ρ_E is

$$\rho_E = \Phi(\rho + \rho_0) \tag{13.8}$$

The term ρ_0 is included because Φ will vary if the y-position of the charge varies. To the first order, the a-c component ρ_E of the effective charge is,

$$\rho_E = \Phi\rho + \rho_0\Phi' y \tag{13.9}$$

$$\rho_E = \Phi\rho - (I_0/u_0)\Phi' y \tag{13.9}$$

Here y is the a-c variation in position along the y coordinate. Thus, if $\Phi \neq 0$, we have instead of (13.7)

$$V = \frac{-j\omega\Gamma_1 K(\Phi\rho - (I_0/u_0)\Phi' y)}{(\Gamma^2 - \Gamma_1^2)}. \tag{13.10}$$

This is the circuit equation we shall use.

13.2 Ballistic Equations

We will assume an unperturbed motion of velocity u_0 in the z direction, parallel to a uniform magnetic focusing field of strength B. As in Chapter II, products of a-c quantities will be neglected.

In the x direction, perpendicular to the y and z directions

$$d\dot{x}/dt = -\eta B\dot{y} \tag{13.11}$$

Assume that $\dot{x} = 0$ at $y = 0$. Then

$$\dot{x} = \eta B y \tag{13.12}$$

In the y direction we have

$$d\dot{y}/dt = \eta(B\dot{x} - E_y) \tag{13.13}$$

From (13.5) this is

$$d\dot{y}/dt = \eta(B\dot{x} + \Phi' V) \tag{13.14}$$

$$d\dot{y}/dt = \partial\dot{y}/\partial t + (\partial\dot{y}/\partial z)(dz/dt) \tag{13.15}$$

$$(d\dot{y}/dt) = u_0(j\beta_e - \Gamma)\dot{y} \tag{13.16}$$

We obtain from (13.16), (13.14) and (13.12)

$$(j\beta_e - \Gamma)y = -u_0\beta_m^2 y + \eta\Phi' V/u_0 \tag{13.17}$$

$$\beta_m = \eta B/u_0 \tag{13.18}$$

Here ηB is the cyclotron radian frequency and β_m is a corresponding propagation constant.

Now

$$\dot{y} = \partial y/\partial t - (\partial y/\partial z)(\partial z/\partial t) \tag{13.19}$$

$$\dot{y} = u_0(j\beta_e - \Gamma)y \tag{13.20}$$

From (13.20) and (13.17) we obtain

$$y = \frac{\Phi' V}{2V_0[(j\beta_e - \Gamma)^2 + \beta_m^2]}. \tag{13.21}$$

It is easily shown that the equation for ρ can be obtained exactly as in Chapter II. From (2.22) and (2.18) we have

$$\rho = \frac{I_0 \Gamma^2 \Phi V}{2u_0 V_0(j\beta_e - \Gamma)^2}. \tag{13.22}$$

13.3 Combined Equation

From the circuit equation (13.10) and the ballistical equations (13.21) and (13.22) we obtain

$$1 = \frac{-j\beta_e \Gamma_1 \Gamma^2 \Phi^2 K I_0}{2V_0(\Gamma^2 - \Gamma_1^2)}\left[\frac{1}{(j\beta_e - \Gamma)^2} - \frac{(\Phi'/\Phi)^2}{\Gamma^2[(j\beta_e - \Gamma)^2 + \beta_m^2]}\right]. \tag{13.23}$$

The voltage at the beam is Φ times the circuit voltage, so the effective impedance of the circuit at the beam is Φ^2 times the circuit impedance. Thus

$$C^3 = \Phi^2 K I_0/4V_0 \tag{13.24}$$

It will be convenient to define a dimensionless parameter f specifying β_m and hence the magnetic field

$$f = \beta_m/\beta_e C \tag{13.25}$$

We will also use δ and b as defined earlier

$$-\Gamma = -j\beta_e + \beta_e C\delta$$

$$-\Gamma_1 = -j\beta_e - j\beta_e C b$$

After the usual approximations, (13.23) yields

$$j\delta - b = \frac{1}{\delta^2} + \frac{\alpha^2}{(\delta^2 + f^2)} \tag{13.26}$$

$$\alpha^2 = (\Phi'/\beta_e\Phi)^2 \tag{13.27}$$

It is interesting to consider the quantity $(\Phi'/\beta_e\Phi)^2$ for typical fields. For

instance, in the two-dimensional electrostatic field in which the potential V is given by

$$V = Ae^{-\beta_e y}e^{-j\beta_e z} \tag{13.28}$$

$$\partial V/\partial y = -\beta_e V \tag{13.29}$$

and everywhere

$$\alpha^2 = (\Phi'/\beta_e\Phi)^2 = 1. \tag{13.30}$$

Relation (13.30) is approximately true far from the axis in an axially symmetrical field.

Consider a potential giving a purely transverse field at $y = 0$

$$V = Ae^{-j\beta_e z}\sinh \beta_e y \tag{13.31}$$

$$\frac{\partial V}{\partial y} = \beta A e^{-j\beta_e z}\cosh \beta_e y. \tag{13.32}$$

In this case, at $y = 0$

$$\alpha^2 = (\Phi'/\beta_e\Phi)^2 = \infty \tag{13.33}$$

In the case of a purely transverse field we let

$$D^3 = \frac{I_0\Phi'^2 K}{4V_0\beta_e^2} \tag{13.34}$$

$$D^3 = (E_y^2/\beta^2 P)(I_0/8V_0) \tag{13.35}$$

In (13.35), E_y is the magnitude of the y component of field for a power flow P, and β is the phase constant.

We then redefine δ and b in terms of D rather than C

$$-\Gamma = -j\beta_e + \beta_e D\delta \tag{13.36}$$

$$-\Gamma_1 = -j\beta_e - j\beta_e Db \tag{13.37}$$

and our equation for a purely transverse field becomes

$$1 = (j\delta - b)(\delta^2 + f^2) \tag{13.38}$$

In (13.38), δ and b are of course not the same as in (13.26) but are defined by (13.36) and (13.37).

13.4 Purely Transverse Fields

The case of purely transverse fields is of interest chiefly because, as was mentioned in Chapter X, it has been suggested that such tubes should have low noise.

In terms of x and y as usually defined

$$\delta = x + jy$$

equation (13.38) becomes

$$x[(x^2 - y^2 + f^2) - 2y(y + b)] = 0 \tag{13.39}$$

$$(y + b)(x^2 - y^2 + f^2) + 2x^2y + 1 = 0 \tag{13.40}$$

From the $x = 0$ solution of (13.39) we obtain

$$x = 0 \tag{13.41}$$

$$b = \frac{1}{y^2 - f^2} - y. \tag{13.42}$$

It is found that this solution obtains for large and small values of b. For very large and very small values of b, either

$$y \doteq -b \tag{13.43}$$

or

$$y \doteq \pm f \tag{13.44}$$

The wave given by (13.43) is a circuit wave; that given by (13.44) represents electrons traveling down the tube and oscillating with the cyclotron frequency in the magnetic field.

In an intermediate range of b, we have from (13.39)

$$x = \pm\sqrt{2y(y + b) - (f^2 - y^2)} \tag{13.45}$$

and

$$b = -2y \pm \sqrt{f^2 - 1/2y}. \tag{13.46}$$

For a given value of f^2 we can assume values of y and obtain values of b. Then, x can be obtained from (13.45). In Figs. 13.5–13.10, x and y are plotted vs. b for $f^2 = 0$, .5, 1, 4 and 10. It should be noted that x_1, the parameter expressing the rate of increase of the increasing wave, has a maximum at larger values of b as f is increased (as the magnetic focusing field is increased). Thus, for higher magnetic focusing fields the electrons must be shot into the circuit faster to get optimum results than for low fields. In Fig. 13.11, the maximum positive value of x is plotted vs. f. The plot serves to illustrate the effect on gain of increasing the magnetic field.

Let us consider an example. Suppose

$$\lambda = 7.5 \text{ cm}$$

$$D = .03$$

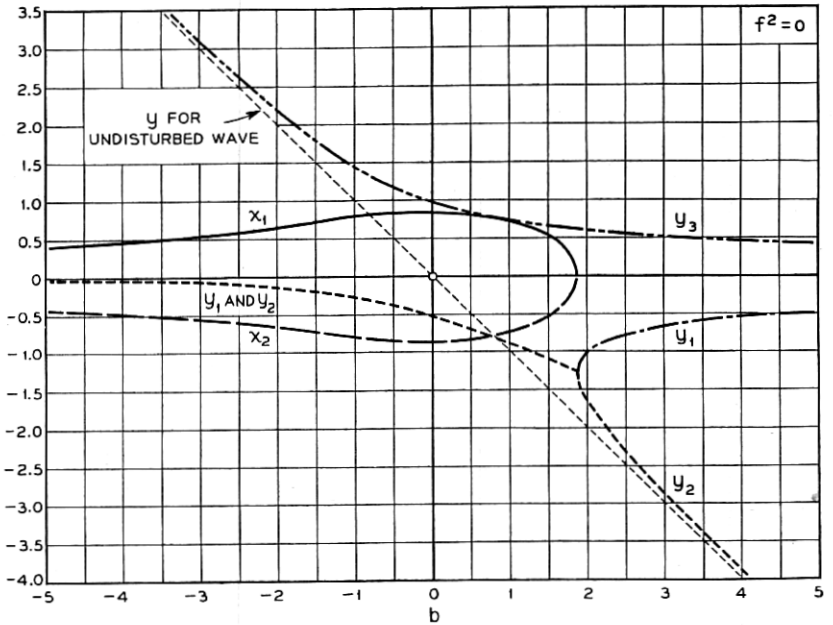

Fig. 13.5—The x's and y's for the three forward waves when the circuit field is purely transverse at the thin electron stream, for zero magnetic focusing field ($f^2 = 0$).

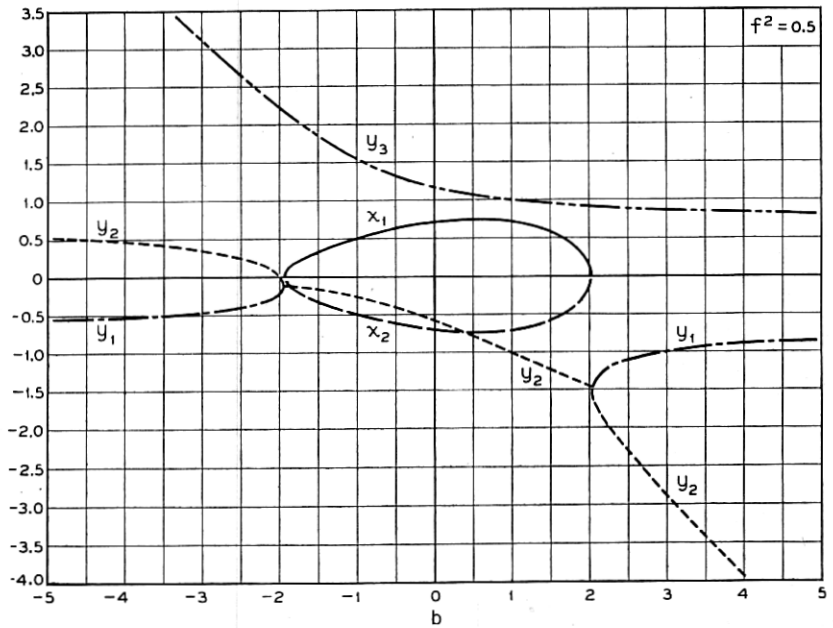

Fig. 13.6—Curves similar to those of Fig. 13.5 for a parameter $f^2 = 1$. The parameter f is proportional to the strength of the magnetic focusing field.

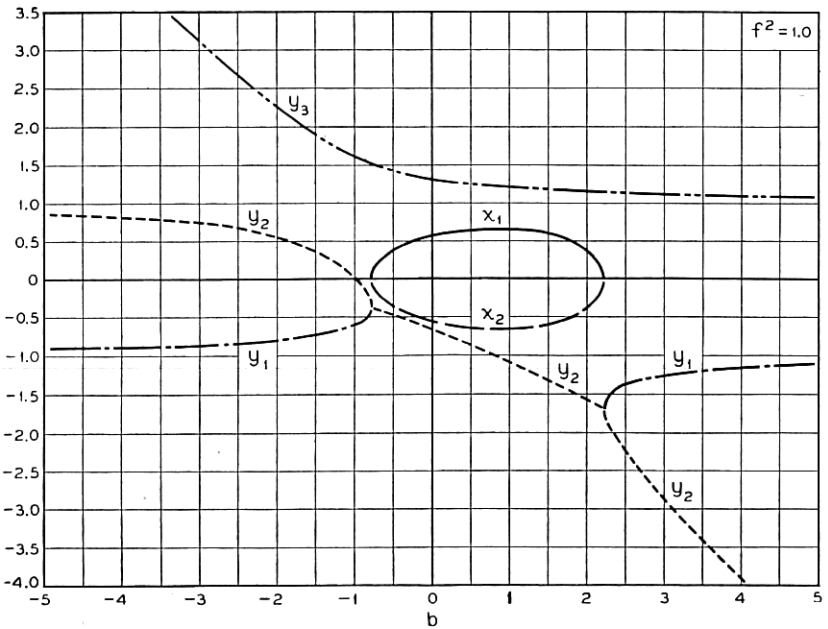

Fig. 13.7—The x's and y's for $f^2 = 1.0$.

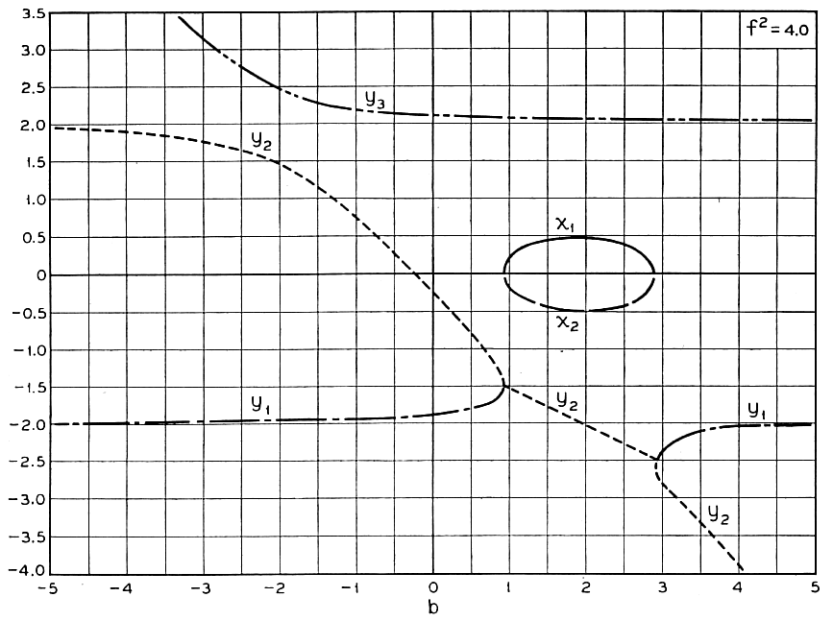

Fig. 13.8—The x's and y's for $f^2 = 2.0$.

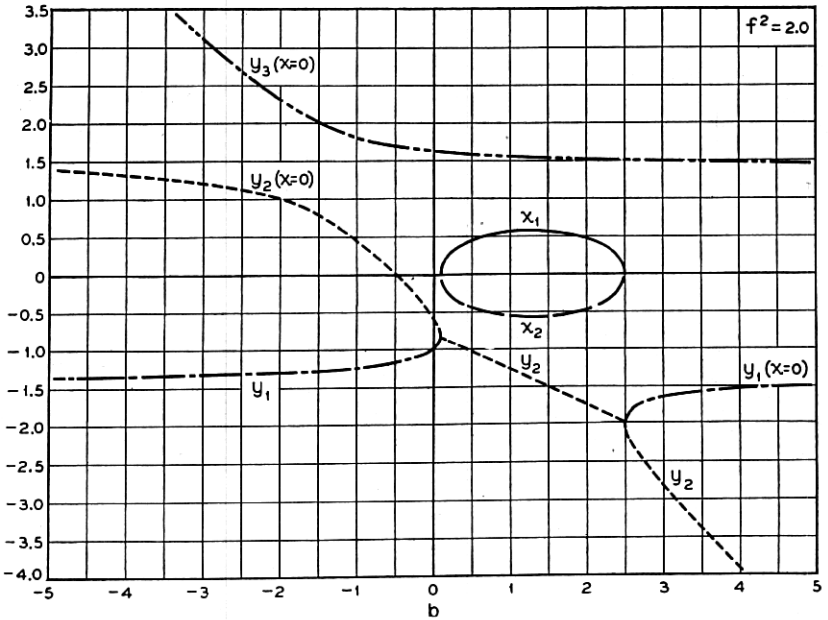

Fig. 13.9—The x's and y's for $f = 4.0$.

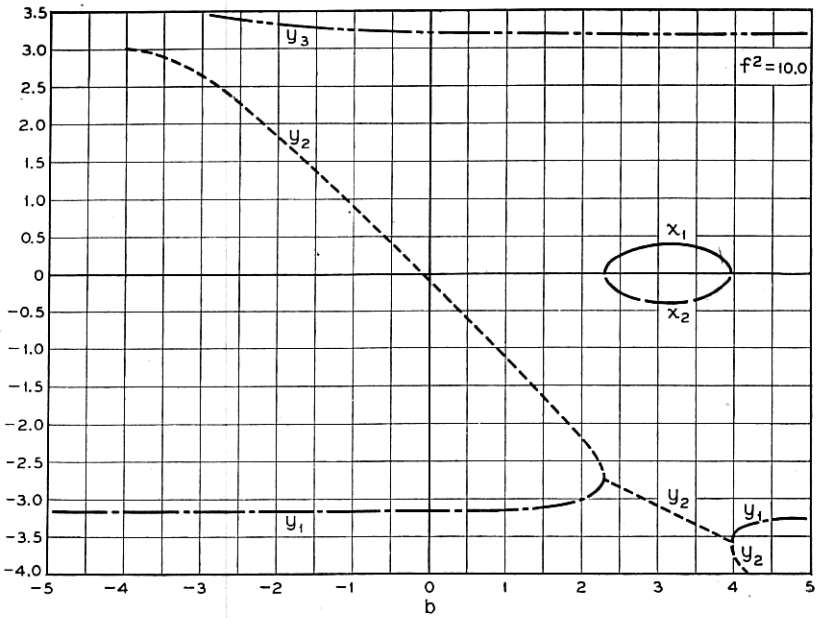

Fig. 13.10—The x's and y's for $f^2 = 10.0$.

These values are chosen because there is a longitudinal field tube which operates at 7.5 cm with a value of C (which corresponds to D) of about .03. The table below shows the ratio of the maximum value of x_1 to the maximum value of x_1 for no magnetic focusing field.

Magnestic Field in Gauss	f	x_1/x_{10}
0	0	1
50	1.17	.71
100	2.34	.50

A field of 50 to 100 gauss should be sufficient to give useful focusing action. Thus, it may be desirable to use magnetic focusing fields in transverse-

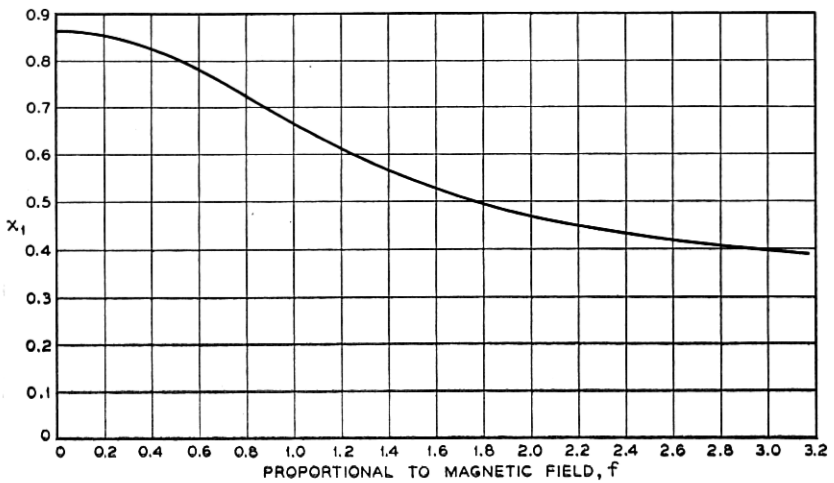

Fig. 13.11—Here x_1, the x for the increasing wave, is plotted vs f, which is proportional to the strength of the focusing field. The velocity parameter b has been chosen to maximize x_1. The ordinate x_1 is proportional to gain per wavelength.

field traveling-wave tubes. This will be more especially true in low-voltage tubes, for which D may be expected to be higher than .03.

13.5 Mixed Fields

In tubes designed for use with longitudinal fields, the transverse fields far off the axis approach in strength the longitudinal fields. The same is true of transverse field tubes far off the axis. Thus, it is of interest to consider equation (13.26) for cases in which α is neither very small nor very large, but rather is of the order of unity.

If the magnetic field is very intense so that f^2 is large, then the term containing α^2, which represents the effect of transverse fields, will be very small and the tube will behave much as if the transverse fields were absent.

Consideration of both terms presents considerable difficulty as (13.26) leads to five waves (5 values of δ) instead of three. The writer has attacked the problem only for the special case of $b = 0$. In this case we obtain from (13.26)

$$\delta = -j\left[\frac{1}{\delta^2} + \frac{\alpha^2}{\delta^2 + f^2}\right] \tag{13.47}$$

MacColl has shown[1] that the two "new" waves (waves introduced when $\alpha = 0$) are unattenuated and thus unimportant and uninteresting (unless, as an off-chance, they have some drastic effect in fitting the boundary conditions).

Proceeding from this information, we will find the change in δ as f^2 is increased from zero. From (13.47) we obtain

$$d\delta = j\left[\frac{2d\delta}{\delta^3} + \frac{2\alpha^2\,\delta d\delta}{(\delta^2+f^2)^2} + \frac{\alpha^2\,df^2}{(\delta^2+f^2)^2}\right] \tag{13.48}$$

Now, if $f = 0$

$$\delta^3 = -j(1 + \alpha^2) \tag{13.49}$$

If we use this in connection with (13.48) we obtain

$$d\delta = -\frac{\alpha^2}{3\delta}\,df^2 \tag{13.50}$$

For an increasing wave

$$\delta_1 = (1 + (\Phi'/\beta_e\Phi)^2)(\sqrt{3}/2 - j/2) \tag{13.51}$$

Hence, for the increasing wave

$$d\delta_1 = \frac{\alpha^2(-\sqrt{3}/2 - j/2)}{3(1 + \alpha^2)}\,df^2 \tag{13.52}$$

This shows that applying a small magnetic field tends to decrease the gain. This does not mean, however, that the gain with a longitudinal and transverse field and a magnetic field is less than the gain with the longitudinal field alone. To see this we assume that not f^2 but $(\Phi'/\beta_e\Phi)^2$ is small. Differentiating, we obtain

$$d\delta = -j\left[-\frac{2d\delta}{\delta^3} - \frac{2\alpha^2\,\delta d\delta}{(\delta^2+f^2)^2} + \frac{d\alpha^2}{\delta^2+f^2}\right] \tag{13.53}$$

If $\alpha = 0$

$$\delta^3 = -j \tag{13.54}$$

[1] J. R. Pierce, "Transverse Fields in Traveling-Wave Tubes," *Bell System Technical Journal*, Vol. 27, pp. 732–746.

and we obtain

$$d\delta = \frac{1}{3}\frac{\delta^3}{(\delta^2 + f^2)}\,d\alpha^2 \tag{13.55}$$

$$d\delta = \frac{-j}{3(\delta^2 + f^2)}\,d\alpha^2 \tag{13.56}$$

If we have a very large magnetic field ($f^2 \gg |\,\delta^2\,|$), then

$$d\delta = \frac{-j}{3f^2}\,d\alpha^2 \tag{13.57}$$

and the change in δ is purely reactive. If $f = 0$ (no magnetic field), from (13.55)

$$d\delta = \frac{\delta}{3}\,d\alpha^2 \tag{13.58}$$

Adding a transverse field component increases the magnitude of δ without changing the phase angle.

CHAPTER XIV

FIELD SOLUTIONS

Synopsis of Chapter

SO FAR, it has been assumed that the same a-c field acts on all electrons. This has been very useful in getting results, but we wonder if we are overlooking anything by this simplification.

The more complicated situation in which the variation of field over the electron stream is taken into account cannot be investigated with the same generality we have achieved in the case of "thin" electron streams. The chief importance we will attach to the work of this chapter is not that of producing numerical results useful in designing tubes. Rather, the chapter relates the appropriate field solutions to those we have been using and exhibits and evaluates features of the "broad beam" case which are not found in the "thin beam" case.

To this end we shall examine with care the simplest system which can reasonably be expected to exhibit new features. The writer believes that this will show qualitatively the general features of most or all "broad beam" cases.

The case is that of an electron stream of constant current density completely filling the opening of a double finned circuit structure, as shown in Fig. 14.1. The susceptance looking into the slots between the fins is a function of frequency only and not of propagation constant. Thus, at a given frequency, we can merely replace the slotted circuit members by susceptance sheets relating the magnetic field to the electric field, as shown in Fig. 14.2. The analysis is carried out with this susceptance as a parameter. Only the mode of propagation with a symmetrical field pattern is considered.

First, the case for zero current density is considered. The natural mode of propagation will have a phase constant β such that H_x/E_z for the central region is the same as H_x/E_z for the finned circuit. The solid curve of Fig. 14.3 shows a quantity proportional to H_x/E_z for the central space vs $\theta = \beta d$ (d defined by Fig. 14.1), a quantity proportional to β. The dashed line P represents H_x/E_z for a given finned structure. The intersections specify values of θ for the natural active modes of propagation to the left and to the right, and, hence, values of the natural phase constants.

The structure also has passive modes of propagation. If we assume fields which vary in the z direction as exp $(\Phi/d)z$, H_x/E_z for the central

opening varies with Φ as shown in part in Fig. 14.4. A horizontal line representing a given susceptance of the finned structure will intersect the curve at an infinite number of points. Each intersection represents a passive mode which decays at a particular rate in the z direction and varies sinusoidally with a particular period in the y direction.

If the effect of the electrons in the central space is included, H_x/E_z for the central space no longer varies as shown in Fig. 14.3, but as shown in Fig. 14.5 instead. The curve goes off to $+\infty$ near a value of θ corresponding to a phase velocity near to the electron velocity. The nature of the modes depends on the susceptance of the finned structure. If this is represented by P_1, there are four unattenuated waves; for P_3 there are two unattenuated waves and an increasing and a decreasing wave. P_2 represents a transitional case.

Not the whole of the curve for the central space is shown on Fig. 14.5. In Fig. 14.6 we see on an expanded scale part of the region about $\theta = 1$, between the points where the curve goes through 0. The curve goes to $+\infty$ and repeatedly from $-\infty$ to $+\infty$, crossing the axis an infinite number of times as θ approaches unity. For any susceptance of the finned structure, this leads to an infinite number of unattenuated modes, which are space-charge waves; for these the amplitude varies sinusoidally with different periods across the beam. Not all of them have any physical meaning, for near $\theta = 1$ the period of cyclic variation across the beam will become small even compared to the space between electrons.

Returning to Fig. 14.1, we may consider a case in which the central space between the finned structures is very narrow (d very small). This will have the effect of pushing the solid curve of Fig. 14.5 up toward the horizontal axis, so that for a reasonable value of P (say, P_1, P_2 or P_3 of Fig. 14.5) there is no intersection. That is, the circuit does not propagate any unattenuated waves. In this case there are still an increasing and a decreasing wave. The behavior is like that of a multi-resonator klystron carried to the extreme of an infinite number of resonators. If we add resonator loss, the behavior of gain per wavelength with frequency near the resonant frequency of the slots is as shown in Fig. 14.7.

One purpose of this treatment of a broad electron stream is to compare its results with those of the previous chapters. There, the treatment considered two aspects separately: the circuit and the effect of the electrons.

Suppose that at $y = d$ in Fig. 14.1 we evaluate not H_x for the finned structure and for the central space separately, but, rather, the difference or discontinuity in H_x. This can be thought of as giving the driving current necessary to establish the field E_z with a specified phase constant. In Fig. 14.8, y_1 is proportional to this H_x or driving current divided by E_z. The dashed curve y_2 is the variation of driving current with θ or β which we have

used in earlier chapters, fitted to the true curve in slope and magnitude at $y = 0$. Over the range of θ of interest in connection with increasing waves, the fit is good.

The difference between H_x/E_z for the central space without electrons (Fig. 14.3) and H_x/E_z for the central space with electrons (Fig. 14.5) can be taken as representing the driving effect of the electrons. The solid curve of Fig. 14.9 is proportional to this difference, and hence represents the true effect of the electrons. The dashed curve is from the ballistical equation used in previous chapters. This has been fitted by adjusting the space-charge parameter Q only; the leading term is evaluated directly in terms of current density, beam width, β, and variation of field over the beam, which is assumed to be the same as in the absence of electrons.

Figure 14.10 shows a circuit curve (as, of Fig. 14.8) and an electronic curve (as, of Fig. 14.10). These curves contain the same information as the curves (including one of the dashed horizontal lines) of Fig. 14.5, but differently distributed. The intersections represent the modes of propagation.

If such curves were the approximate (dashed) curves of Figs. 14.8 and 14.9, the values of θ for the modes would be quite accurate for real intersections. It is not clear that "intersections" for complex values of θ would be accurately given unless they were for near misses of the curves. In addition, the complicated behavior near $\theta = 1$ (Fig. 14.6) is quite absent from the approximate electronic curve. Thus, the approximate electronic curve does not predict the multitude of unattenuated space-charge waves near $\theta = 1$. Further, the approximate expressions predict a lower limiting electron velocity below which there is no gain. This is not true for the exact equations when the electron flow fills the space between the finned structures completely.

It is of some interest to consider complex intersections in the case of near misses by using curves of simple form (parabolas), as in Fig. 14.11. Such an analysis shows that high gain is to be expected in the case of curves such as those of Fig. 14.10, for instance, when the circuit curve is not steep and when the curvature of the electronic curve is small. In terms of physical parameters, this means a high impedance circuit and a large current density.

14.1 The System and the Equations

The system examined is a two-dimensional one closely analogous to that of Fig. 4.4. It is shown in Fig. 14.1. It consists of a central space extending from $y = -d$ to $y = +d$, and arrays of thin fins separated by slots extending for a distance h beyond the central opening and short-circuited at the outer ends. An electron flow of current density J_0 amperes/m^2 fills the open space. It is assumed that the electrons are constrained by a strong magnetic field so that they can move in the z direction only.

We can simplify the picture a little. The open edges of the slots merely form impedance sheets.

From 4.12 we see that at $y = -d$

$$\frac{H_x}{E_z} = \frac{j\omega\epsilon}{\beta_0} \cot \beta_0 h \tag{14.1}$$

$$\frac{H_x}{E_z} = -jB \tag{14.2}$$

$$B = -\sqrt{\epsilon/\mu} \cot \beta_0 h \tag{14.3}$$

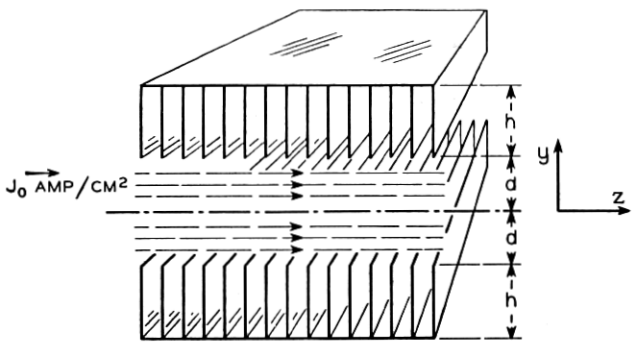

Fig. 14.1—Electron flow completely fills the open space between two finned structures. A strong axial magnetic field prevents transverse motions.

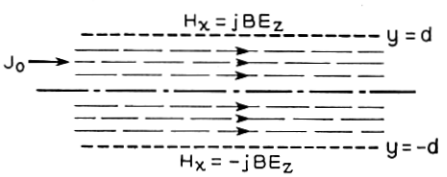

Fig. 14.2—In analyzing the structure of Fig. 14.1, the finned members are regarded as susceptance sheets.

for

$$\beta_0/\omega\epsilon = 1/c\epsilon = \sqrt{\mu/\epsilon} = 377 \text{ ohms} \tag{14.4}$$

Similarly, at $y = +d$,

$$\frac{H_x}{E_z} = jB \tag{14.5}$$

We can use B as a parameter rather than h. Thus, we obtain the picture of Fig. 14.2. This picture is really more general than Fig. 14.1, for it applies for any transverse-magnetic circuit outside of the beam.

Inside of the beam the effect of the electrons is to change the effective dielectric constant in the z direction. Thus, from (2.22) we have for the electron convection current

$$i = \frac{jJ_0\beta_e\Gamma V}{2V_0(j\beta_e - \Gamma)^2} \tag{2.22}$$

Now

$$E_z = -\frac{\partial V}{\partial z} = \Gamma V \tag{14.6}$$

so that

$$i = \frac{jJ_0\beta_e E_z}{2V_0(j\beta_e - \Gamma)^2} \tag{14.7}$$

The appearance of a voltage V in (2.22) and (14.6) does not mean that these relations are invalid for fast waves. In (2.22) the only meaning which need be given to V is that defined by (14.6), as it is the electric field as specified by (14.6) that was assumed to act on the electrons in deriving (2.22).

Let us say that the total a-c current density in the z direction, J_z, is

$$J_z = j\omega\epsilon_1 E_z \tag{14.8}$$

This current consists of a displacement current $j\omega\epsilon E_z$ and the current i, so that

$$J_z = j\omega\epsilon_1 E_z = j\omega\epsilon E_z\left(1 + \frac{J_0\beta_e}{2\epsilon\omega V_0(j\beta_e - \Gamma)^2}\right) \tag{14.9}$$

Hence

$$\epsilon_1/\epsilon = \left(1 + \frac{J_0\beta_e}{2\epsilon\omega V_0(j\beta_e - \Gamma)^2}\right) \tag{14.10}$$

This gives the ratio of the effective dielectric constant in the z direction to the actual dielectric constant. We will proceed to put this in a form which in the long run will prove more convenient.

Let us define a quanity β

$$\Gamma = j\beta \tag{14.11}$$

and a quantity A

$$A = \frac{J_0 d^2}{2\epsilon u_0 V_0} \tag{14.12}$$

And quantities θ and θ_e

$$\theta_e = \beta_e d = (\omega/u_0)d \tag{14.13}$$

$$\theta = \beta d \tag{14.14}$$

We recognize d as the half-width of the opening filled by electrons. Then

$$\epsilon_1/\epsilon = 1 - \frac{A}{(\theta_e - \theta)^2} \tag{14.15}$$

We can say something about the quantity A. From purely d-c considerations, the electron flow will cause a fall in d-c potential toward the center of the beam. Indeed, this is so severe for large currents that it sets a limit to the current density which can be transmitted. If we take V_0 and u_0 as values at $y = \pm d$ (the wall), the maximum value of A as defined by (14.12) is 2/3, and at this maximum value the potential at $y = 0$ is $V_0/4$. This is inconsistent with the analysis, in which V_0 and u_0 are assumed to be constant across the electron flow. Thus, for the current densities for which the analysis is valid, which are the current densities such as are usually used in traveling-wave tubes

$$A \ll 1 \tag{14.16}$$

In the a-c analysis we will deal here only with the symmetrical type of wave in which $E_z(+y) = E_z(-y)$. The work can easily be extended to cover cases for which $E_z(+y) = -E_z(-y)$. We assume

$$H_x = H_0 \sinh \gamma y e^{-j\beta z} \tag{14.17}$$

From Maxwell's equations

$$j\omega\epsilon E_y = \frac{\partial H_x}{\partial z} = -j\beta H_0(\sinh \gamma y)e^{-j\beta z}$$

$$E_y = -\frac{\beta}{\omega\epsilon} H_0(\sinh \lambda y)e^{-j\beta z} \tag{14.18}$$

Similarly

$$j\omega\epsilon_1 E_z = -\frac{\partial H_x}{\partial y} = -\gamma H_0(\cosh \gamma y)e^{-j\beta z}$$

$$E_z = \frac{j\gamma}{\omega\epsilon_1} H_0(\cosh \gamma y)e^{-j\beta z} \tag{14.19}$$

We must also have

$$-j\omega\mu H_x = \frac{\partial E_z}{\partial y} - \frac{\partial E_y}{\partial z}$$

$$-j\omega\mu H_0 e^{-j\beta z} \sinh \gamma y = \frac{j\gamma^2}{\omega\epsilon_1} H_0 e^{-j\beta z} \cosh \gamma y - \frac{j\beta^2}{\omega\epsilon} H_0 e^{-j\beta z} \sinh \gamma y$$

$$\gamma^2 = (\epsilon_1/\epsilon)(\beta^2 - \beta_0^2) \tag{14.20}$$

$$\beta_0^2 = \omega^2\mu\epsilon = \omega^2/c^2 \tag{14.21}$$

Now, from (14.17), (14.19) and (14.20)

$$\frac{H_x}{E_z} = \frac{-j\omega\epsilon(\epsilon_1/\epsilon)\tanh\,[(\epsilon_1/\epsilon)^{1/2}(\beta^2-\beta_0^2)^{1/2}\,y]}{(\epsilon_1/\epsilon)^{1/2}(\beta^2-\beta_0^2)^{1/2}} \tag{14.22}$$

But

$$\omega\epsilon = (\omega/c)(c\epsilon) = \beta_0\sqrt{\epsilon/\mu} \tag{14.23}$$

Hence

$$\frac{H_x}{E_z} = \frac{-j\sqrt{\epsilon/\mu}(\epsilon_1/\epsilon)^{1/2}\beta_0\tanh\,[(\epsilon_1/\epsilon)^{1/2}(\beta^2-\beta_0^2)^{1/2}y]}{(\beta^2-\beta_0^2)^{1/2}} \tag{14.24}$$

At $y = d$, (14.5) must apply. From (14.24) we can write

$$P = -\frac{(\epsilon_1/\epsilon)^{1/2}\tanh\,[(\epsilon_1/\epsilon)^{1/2}(\theta^2-\theta_0^2)^{1/2}]}{(\theta^2-\theta_0^2)^{1/2}} \tag{14.25}$$

Here θ is given by (14.14)

$$\theta_0 = \beta_0 d = (\omega/c)d \tag{14.26}$$

and P is given by

$$P = B/\beta_0 d\sqrt{\epsilon/\mu} = B/\theta_0\sqrt{\epsilon/\mu} \tag{14.27}$$

Thus, θ_0 expresses d in radians at free-space wavelength and P is a measure of the wall reactance, the susceptance rising as B rises.

14.2 Waves in the Absence of Electrons

In this section we will consider (14.25) in the case in which there are no electrons and $\epsilon_1/\epsilon = 1$. In this case (14.25) becomes

$$P = -\frac{\tanh\,(\theta^2-\theta_0^2)^{1/2}}{(\theta^2-\theta_0^2)^{1/2}} \tag{14.28}$$

Suppose we plot the right-hand side of (14.28) vs θ for real values of θ_1 corresponding to unattenuated waves. In Fig. 14.3 this has been done for $\theta_0 = 1/10$. For $\theta_0 > \pi/2$ the behavior near the origin is different, but in cases corresponding to actual traveling wave tubes $\theta_0 < \pi/2$.

Intersections between a horizontal line at height P and the curve give values of θ representing unattenuated waves. We see that for the case which we have considered, in which $\theta_0 < \pi/2$ and $\theta_0 \cot \theta_0 > 1$, there are unattenuated waves if

$$P > -\tan\theta_0/\theta_0 \tag{14.29}$$

For $P = -\infty$ (no slot depth and no wall reactance) the system for $\theta_0 < \pi/2$ constitutes a wave guide operated below cutoff frequency for the type of

wave we have considered. If we increase P ($|P|$ decreasing; the inductive reactance of the walls increasing) this finally results in the propagation of a wave. There are two intersections, at $\theta = \pm\theta_1$, representing propagation to the right and propagation to the left. The variation of θ_1 with P is such that as P is increased (made less negative) θ_1 is increased; that is, the greater is P (the smaller $|P|$), the more slowly the wave travels.

There is another set of waves for which θ is imaginary; these represent passive modes which do not transmit energy but merely decay with distance. In investigating these modes we will let

$$\theta = j\Phi \tag{14.30}$$

so that the waves vary with z as

$$e^{(\Phi/d)z} \tag{14.31}$$

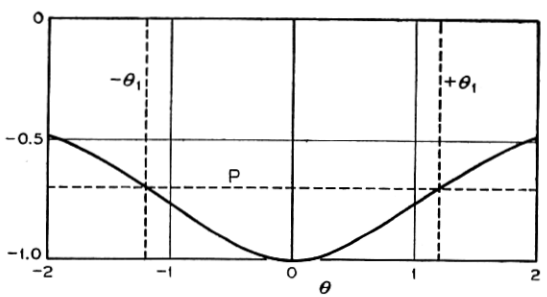

Fig. 14.3—The structure of Fig. 14.1 is first analyzed in the absence of an electron stream. Here a quantity proportional to H_x/E_x at the susceptance sheet is plotted vs $\theta = \beta d$, a quantity proportional to the phase constant β. The solid curve is for the inner open space; the dashed line is for the susceptance sheet. The two intersections at $\pm\theta_1$ correspond to transmission of a forward and a backward wave.

Now (14.28) becomes

$$P = -\tan(\Phi^2 + \theta_0^2)^{1/2}/(\Phi^2 + \theta_0^2)^{1/2} \tag{14.32}$$

In Fig. 14.4 the right-hand side of (14.28) has been plotted vs Φ, again for $\theta_0 = 1/10$.

Here there will be a number of intersections with any horizontal line representing a particular value of P (a particular value of wall susceptance), and these will occur at paired values of Φ which we shall call $\pm\Phi_n$. The corresponding waves vary with distance as $\exp(\pm\Phi_n z/d)$.

Suppose we increase P. As P passes the point $-(\tan\theta_0)/\theta_0$, Φ^n for a pair of these passive waves goes to zero; then for P just greater than $-(\tan\theta_0)/\theta_0$ we have two active unattenuated waves, as may be seen by comparing Figs. 14.4 and 14.3.

14.3 Waves in the Presence of Electrons

In this section we deal with the equations

$$P = \frac{-(\epsilon_1/\epsilon)^{1/2} \tanh [(\epsilon_1/\epsilon)^{1/2}(\theta^2 - \theta_0^2)^{1/2}]}{(\theta^2 - \theta_0^2)^{1/2}} \tag{14.25}$$

and

$$\epsilon_1/\epsilon = 1 - \frac{A}{(\theta_e - \theta)^2} \tag{14.15}$$

We consider cases in which the electron velocity is much less than the velocity of light; hence

$$\theta_e \gg \theta_0 \tag{14.33}$$

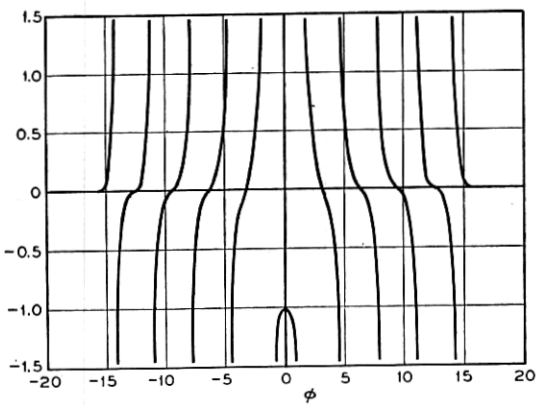

Fig. 14.4—If a quantity proportional to H_x/E_z at the edge of the central region is plotted vs $\Phi = -j\theta$, this curve is obtained. There are an infinite number of intersections with a horizontal line representing the susceptance of the finned structure. These correspond to passive modes, for which the field decays exponentially with distance away from the point of excitation.

In Fig. 14.5, the right-hand side of (14.25) has been plotted vs. θ for $\theta_e = 10\ \theta_0$, corresponding to an electron velocity 1/10 the speed of light. Values of $\theta = 1/10$ and $A = 1/100$ have been chosen merely for convenience.* The curve has not been shown in the region from $\theta = .9$ to $\theta = 1.1$, where ϵ_1/ϵ is negative, and this region will be discussed later.

For a larger value of $P(|P|$ small), P_1 in Fig. 14.5, there are 4 intersections corresponding to 4 unattenuated waves. The two outer intersections obviously correspond to the "circuit" waves we would have in the absence of electrons. The other two intersections near $\theta = .9\theta_e$ and $\theta = 1.1\theta_e$ we call electronic or space-charge waves.

* At a beam voltage $V_0 = 1{,}000$ and for $d = 0.1$ cm, $A = 1/100$ means a current density of about 330 ma/cm², which is a current density in the range encountered in practice.

For instance, increasing P to values larger than P_1 changes θ for the circuit waves a great deal but scarcely alters the two "electronic wave" values of θ, near $\theta = \theta_e(1 \pm 0.1)$. On the other hand, for large values of P the values of θ for the electronic waves are approximately

$$\theta = \theta_e \pm \sqrt{A} \tag{14.34}$$

Thus, changing A alters these values, but changing A has little effect on the values of θ for the circuit waves.

Now, the larger the P the slower the circuit wave travels; and, hence, for large values of P the electrons travel faster than the circuit wave. Our narrow-beam analysis also indicated two circuit waves and two unattenuated electronic waves for cases in which the electron speed is much larger than the speed of the increasing wave. It also showed, however, that, as the difference between the electron speed and the speed of the unperturbed

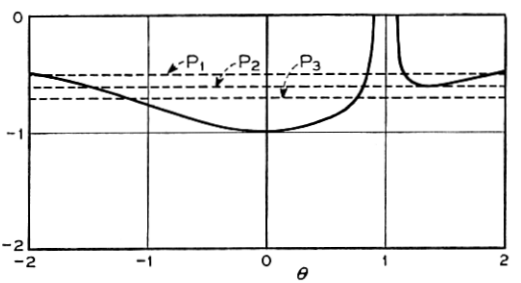

Fig. 14.5—When electrons are present in the open space of the circuit of Fig. 14.1, the curves of Fig. 14.3 are modified as shown here. The nature of the waves depends on the relative magnitude of the susceptance of the finned structure, which is represented by the dashed horizontal lines. For P_1, there are four unattenuated waves, for P_3, two unattenuated waves and an increasing wave and a decreasing wave. Line P_2 represents a transition between the two cases.

wave was made less, a pair of waves appeared, one increasing and one decreasing. This is also the case in the broad beam case.

In Fig. 14.5, when P is given the value indicated by P_2, an "electronic" wave and a "circuit" wave coalesce; this corresponds to y_1 and y_2 running together at $b = (3/2)(2)^{1/3}$ in Fig. 8.1. For a somewhat smaller value of P, such as P_3, there will be a pair of complex values of θ corresponding to an increasing wave and a decreasing wave. We may expect the rate of increase at first to rise and then to fall as P is gradually decreased from the value P_2, corresponding to the rise and fall of x_1 as b is decreased from $(3/2)(2)^{1/3}$ in Fig. 8.1.

It is interesting to know whether or not these increasing waves persist down to $P = -\infty$ (no inductance in the walls). When $P = -\infty$, the only way (14.25) can be satisfied is by

$$\coth\left((\epsilon_1/\epsilon)^{1/2}(\theta^2 - \theta_0^2)^{1/2}\right) = 0 \tag{14.35}$$

This will occur only if

$$(\epsilon_1/\epsilon)^{1/2}(\theta^2 - \theta_0^2)^{1/2} = j\left(n\pi + \frac{\pi}{2}\right)$$
$$(\epsilon_1/\epsilon)(\theta^2 - \theta_0^2) = -\left(n\pi + \frac{\pi}{2}\right)^2 \tag{14.36}$$

Let

$$\theta = u + jw \tag{14.37}$$

From (14.37), (14.36) and (14.15)

$$\left[1 - \frac{A}{((\theta_e - u) + jw)^2}\right]((u + jw)^2 - \theta_0^2) = -\left(n\pi + \frac{\pi}{2}\right)^2 \tag{14.38}$$

If we separate the real and imaginary parts, we obtain

$$[(A - 1)(\theta_e - u)^2 - (A + 1)w^2](u^2 - w^2 - \theta_0^2)$$
$$- 4Auw^2(\theta_e - u) = [(\theta_e - u)^2 + w^2]\left(n\pi + \frac{\pi}{2}\right)^2 \tag{14.39}$$

$$w(u[(\theta_e - u)^2 + w^2] - A[(\theta_e - u)^2 - w^2] + (\theta_e - u)(u^2 - w^2 - \theta_0^2)) = 0 \tag{14.40}$$

The right-hand side of (14.39) is always positive. Because always $A < 1$, the first term on the left of (14.39) is always negative if $u^2 > (w^2 + \theta_0^2)$, which will be true for slow rates of increase. Thus, for very small values of w, (14.39) cannot be satisfied. Thus, it seems that there are no waves such as we are looking for, that is, slow waves ($u \ll c$). It appears that the increasing waves must disappear or be greatly modified when P approaches $-\infty$.

So far we have considered only four of the waves which exist in the presence of electrons. A whole series of unattenuated electron waves exist in the range

$$\theta_e - \sqrt{A} < \theta < \theta_e + \sqrt{A}$$

In this range $(\epsilon_1/\epsilon)^{1/2}$ is imaginary, and it is convenient to rewrite (14.25) as

$$P = \frac{(-\epsilon_1/\epsilon)^{1/2} \tan [(-\epsilon_1/\epsilon)^{1/2}(\theta^2 - \theta_0^2)^{1/2}]}{(\theta^2 - \theta_0^2)^{1/2}} \tag{14.41}$$

The chief variation in this expression over the range considered is that due to variation in $(-\epsilon_1/\epsilon)^{1/2}$. For all practical purposes we may write

$$P = \frac{(-\epsilon_1/\epsilon)^{1/2} \tan [(-\epsilon_1/\epsilon)^{1/2}(\theta_e^2 - \theta_0)^{1/2}]}{(\theta_e^2 - \theta_0^2)^{1/2}} \tag{14.42}$$

Near $\theta = \theta_e$, the tangent varies with infinite rapidity, making an infinite number of crossings of the axis.

In Fig. 14.6, the right-hand side of (14.41) has been plotted for a part of the range $\theta = 0.90\,\theta_e$ to $\theta = 1.10\,\theta_e$. The waves corresponding to the intersections of the rapidly fluctuating curve with a horizontal line representing P are unattenuated space-charge waves. The nearer θ is to θ_e, the larger $(-\epsilon_1/\epsilon)$ is. The amplitude of the electric field varies with y as

$$\cosh\,(j(-\epsilon_1/\epsilon)^{1/2}(\beta^2 - \beta_0^2)^{1/2}y) = \cos\,((-\epsilon_1/\epsilon)^{1/2}(\beta^2 - \beta_0^2)^{1/2}y) \quad (14.45)$$

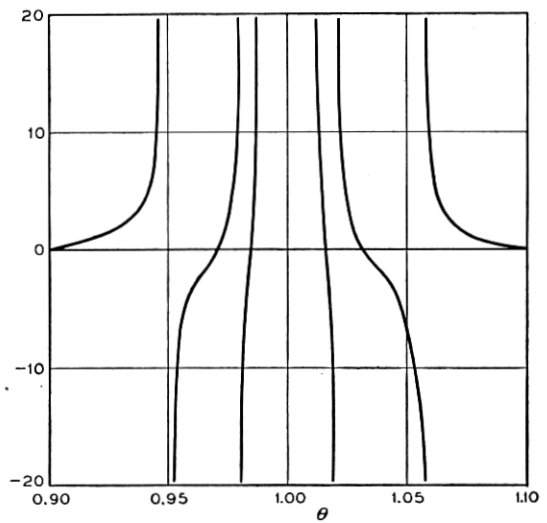

Fig. 14.6—The curve for the central region is not shown completely in Fig. 14.5. A part of the detail around $\theta = 1$, which means a phase velocity equal to the electron velocity, is shown in Fig. 14.6. The curve crosses the axis, and any other horizontal line, an infinite number of times (only some of the branches are shown). Thus, there is a large number of unattenuated "space charge" waves. For these, the amplitude varies sinusoidally in the y direction. Some of these have no physical reality, because the wavelength in the y direction is short compared with the space between electrons.

For small values of $|\theta - \theta_e|$ the field fluctuates very rapidly in the y direction, passing through many cycles between $y = 0$ and $y = d$. For very small values of $|\theta - \theta_e|$ the solution does not correspond to any actual physical problem: spreads in velocity in any electron stream, and ultimately the discrete nature of electron flow, preclude the variations indicated by (14.45).

The writer cannot state definitely that there are not increasing waves for which the real part of θ lies between $\theta_e - \sqrt{A}$ and $\theta_e + \sqrt{A}$, but he sees no reason to believe that there are.

There are, however, other waves which exhibit both attenuation and

propagation. The roots of (14.32) are modified by the introduction of the electrons. To show this effect, let Φ_n be a solution of (14.32), and $j(\Phi_n + \delta)$ be a solution of (14.25). The waves considered will thus vary with distance as

$$e^{[(\Phi_n+\delta)/d]z} \tag{14.43}$$

We see that we must have

$$\begin{aligned}(\epsilon_1/\epsilon)^{1/2}\,(\Phi_n^2 + \theta_0^2)^{1/2}\,\cot\,(\Phi_n^2 + \theta_0^2)^{1/2} \\ = ((\Phi_n + \delta)^2 + \theta_0^2)^{1/2}\,\cot\,[(\epsilon_1/\epsilon)^{1/2}((\Phi_n + \delta)^2 + \theta_0^2)^{1/2}]\end{aligned} \tag{14.44}$$

$$(\epsilon_1/\epsilon)^{1/2} = \left(1 - \frac{A}{(\theta_e - j\Phi_n + \delta)^2}\right)^{1/2} \tag{14.15a}$$

As $A \ll 1$, it seems safe to neglect δ in (14.15a) and to expand, writing

$$(\epsilon_1/\epsilon)^{1/2} = 1 - \alpha \tag{14.46}$$

$$\alpha = \frac{A}{2(\theta_e - j\Phi_n)^2} = \frac{A[(\theta_e^2 - \Phi_n^2) + 2j\theta_e\Phi_n]}{2(\theta_e^2 + \Phi_n^2)^2} \tag{14.47}$$

If $|\,\delta\,| \ll \Phi_n$, we may also write

$$((\Phi_n + \delta)^2 + \theta_0^2)^{1/2} = \frac{\Phi_n\,\delta}{(\Phi_n^2 + \theta_0^2)^{1/2}} + (\Phi_n^2 + \theta_0^2)^{1/2} \tag{14.48}$$

We thus obtain, if we neglect products of δ and α

$$\begin{aligned}(1 - \alpha)\,\cot\,(\Phi_n^2 + \theta_0^2)^{1/2} = \left[1 + \frac{\Phi_n\,\delta}{(\Phi_n^2 + \theta_0^2)^{1/2}}\right]\cot\,(\Phi_n^2 + \theta_0^2)^{1/2} \\ - \left(\frac{\Phi_n\,\delta}{(\Phi_n^2 + \theta_0^2)^{1/2}} - \alpha\right)\csc^2\,(\Phi_n^2 + \theta_0^2)^{1/2}\end{aligned} \tag{14.49}$$

Solving this for δ, we obtain

$$\delta = -\frac{(\Phi_n^2 + \theta_0^2)^{1/2}}{\Phi_n}\left[\frac{\cos\,(\Phi_n^2 + \theta_0^2)^{1/2} + \csc\,(\Phi_n^2 + \theta_0^2)^{1/2}}{\cos\,(\Phi_n^2 + \theta_0^2)^{1/2} - \csc\,(\Phi_n^2 + \theta_0^2)^{1/2}}\right]\alpha \tag{14.50}$$

$$\begin{aligned}\delta = \left[\frac{(\theta_e^2 - \Phi_n^2)}{\Phi_n(\theta_e^2 + \Phi_n^2)^2} + j\,\frac{2\theta_e}{(\theta_e^2 + \Phi_n^2)^2}\right] \\ \cdot \left[\frac{\csc^2\,(\Phi_n^2 + \theta_0^2)^{1/2} + \cos\,(\Phi_n^2 + \theta_0^2)^{1/2}}{\csc\,(\Phi_n^2 + \theta_0^2)^{1/2} - \cos\,(\Phi_n^2 + \theta_0^2)^{1/2}}\right]\frac{A(\theta_0^2 + \Phi_n^2)^{1/2}}{2}\end{aligned} \tag{14.51}$$

As the waves vary with distance as $\exp\,[(\pm\,\Phi_n + \delta)z/d]$, this means that all modified waves travel in the $-z$ direction, and very fast, for the imaginary part of δ, which is inversely proportional to the phase velocity, will be small.

These backward-traveling waves cannot give gain in the $+z$ direction, and could give gain in the $-z$ direction only under conditions similar to those discussed in Chapter XI.

14.4 A Special Type of Solution

Consider (14.25) in a case in which

$$\theta_0 \ll \theta_e \tag{14.52}$$

$$\theta_e \ll 1 \tag{14.53}$$

In this case in the range

$$\theta < \theta_e - \sqrt{A} \quad \text{and} \quad \theta > \theta_e + \sqrt{A} \tag{14.54}$$

we can replace the hyperbolic tangent by its argument, giving

$$P = -(\epsilon_1/\epsilon) = \frac{A}{(\theta_e - \theta)^2} - 1. \tag{14.55}$$

This can be solved for θ, giving

$$\theta = \theta_e \mp \sqrt{A/(P+1)} \tag{14.56}$$

If

$$P < -1$$

Then θ will be complex and there will be a pair of waves, one increasing and one decreasing. We note that, under these circumstances, there is no circuit wave, either with or without electrons.

What we have is in essence an electron stream passing through a series of inductively detuned resonators, as in a multi-resonator klystron. Thus, the structure is in essence a distributed multi-resonator klystron, with lossless resonators. If the resonators have loss, we can let

$$P = (-jG + B)/\theta_0\sqrt{\epsilon/\mu} \tag{14.57}$$

where G is the resonant conductance of the slots. In this case, (14.56) becomes

$$\theta = \theta_e \pm \left(\frac{A\theta\sqrt{\epsilon/\mu}}{-jG + (B + \theta_0\sqrt{\epsilon/\mu})}\right)^{1/2} \tag{14.58}$$

Near resonance we can assume G is a constant and that B varies linearly with frequency. Accordingly, we can show the form of the gain of the increasing wave by plotting vs. frequency the quantity g

$$g = \text{Im}(-j + \omega/\omega_0)^{-1/2} \tag{14.59}$$

In Fig. 14.7, g is plotted vs. ω/ω_0.

Thus, if we wish we may write (14.70) in the form

$$P_e = -\frac{\tanh \theta}{\theta} - P \tag{14.72}$$

where

$$P_e = (1/\theta)[(\epsilon_1/\epsilon)^{1/2} \tanh [(\epsilon_1/\epsilon)^{1/2} \theta - \tanh \theta] \tag{14.73}$$

The quantities on the right of (14.72) refer to the circuit in the absence of electrons; if there are no electrons $P_e = 0$ and (14.72) yields the circuit

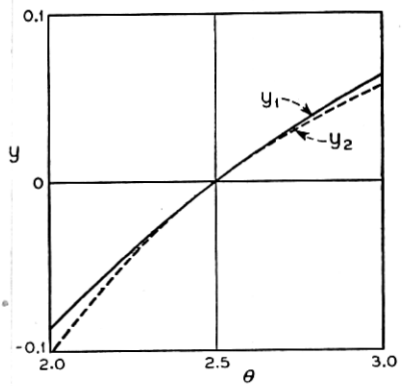

Fig. 14.8—Suppose we compare the circuit admittance for the structure of Fig. 14.1 with that used in earlier calculations. Here the solid curve is proportional to the difference of the H_x's for the finned structure and for the central space (the impressed current) divided by E_z. The dashed curve is the simple expression (6.1) used earlier fitted in magnitude and slope.

waves. Thus, P_e may be regarded as the equivalent of an added current i at the wall, such that

$$\frac{i}{jE_z} = \theta \sqrt{\epsilon/\mu}\, P_e \tag{14.74}$$

Now, the root giving the increasing wave, the one we are most interested in, occurs a little way from the pole, where $(\epsilon_1/\epsilon)^{1/2}$ may be reasonably large if θ is large. It would seem that one of the best comparisons which could be made would be that between the approximate analysis and a very broad beam case, for which θ is very large. In this case, we may take approximately, away from $\theta = \theta_e$

$$\tanh [(\epsilon_1/\epsilon)^{1/2} \theta] = \tanh \theta = 1 \tag{14.75}$$

$$P_e = (1/\theta)[(\epsilon_1/\epsilon)^{1/2} - 1$$

$$P_e = (1/\theta)\left[\left(1 - \frac{A}{(\theta_e - \theta)^2}\right)^{1/2} - 1\right] \tag{14.76}$$

Let us expand in terms of the quantity $A/(\theta_e - \theta)^2$, assuming this to be small compared with unity. We obtain

$$P_e = \frac{A}{2\theta(\theta_e - \theta)^2}\left[1 + \frac{A}{4(\theta_e - \theta)^2} + \cdots\right] \tag{14.77}$$

The theory of Chapter VII is developed by assuming that all electrons are acted on by the same a-c field. When this is not so, it is applied approximately by using an "effective current" or "effective field" as in Chapter IV; either of these concepts leads to the same averaging over the electron flow. An effective current can be obtained by averaging over the flow the current density times the square of the field, evaluated in the absence of electrons, and dividing by the square of the field at the reference position. This is equivalent to the method used in evaluating the effective field in Chapter III.

In the device of Fig. 14.2, if we take as a reference position $y = \pm d$, the effective current I_0 per unit depth

$$I_0 = \frac{J_0 \int_0^d \cosh^2(\gamma y)\, dy}{\cosh^2 \gamma d} \tag{14.78}$$

$$I_0 = (Jd/2)\left(\frac{\tanh \gamma d}{\gamma d} + \operatorname{sech}^2 \gamma d\right) \tag{14.79}$$

This is the effective current associated with the half of the flow from $y = 0$ to $y = d$. Here γ is the value for no electrons. For $\theta \ll \beta$, $\gamma = \beta$. For large values of θ, then

$$I_0 = J_0 d/2\theta \tag{14.80}$$

Now, the corresponding a-c convection current per unit depth will be:

$$i = -j\frac{I_0 \beta_e}{2V_0(\beta_e - \beta)^2} E \tag{14.81}$$

Here E is the total field acting on the electrons in the z-direction. From (7.1) we see that we assumed this to be the field due to the circuit (the first term in the brackets) plus a quantity which we can write

$$E_{z1} = \frac{j\beta^2}{\omega C_1} i \tag{14.82}$$

Accordingly

$$E = E_z + E_{z1} \tag{14.83}$$

and we can write i

$$i = -j \frac{I_0 \beta_e}{2V_0(\beta_e - \beta)^2} \left(E_z + \frac{j\beta^2}{\omega C_1} i \right) \tag{14.84}$$

$$i = \frac{jI_0 \theta_e \, dE_z}{2V_0[K - (\theta_e - \theta)^2]} \tag{14.85}$$

Here K is a parameter specifying the value of $\beta^2/\omega C_1$. As (14.85) need hold over only a rather small range of β, and C is not independent of β, we will regard K as a constant.

The parameter P_e corresponding to (14.85) is

$$P_e = \frac{I_0 \, d(\theta_e/\theta_0)}{2\sqrt{\epsilon/\mu}\, V_0} [K - (\theta_e - \theta)^2]^{-1} \tag{14.86}$$

Now, from (14.80), for large values of θ

$$\frac{I_0 \, d(\theta_e/\theta_0)}{2\sqrt{\epsilon/\mu}\, V_0} = \frac{J_0 \, d^2(\theta_e/\theta_0)}{4\sqrt{\epsilon/\mu}\, \theta V_0} \tag{14.87}$$

As

$$\sqrt{\epsilon/\mu} = \epsilon/\sqrt{\mu\epsilon} = \epsilon c,$$

$$\theta_e/\theta_0 = c/u_0,$$

and

$$A = \frac{J_0 \, d^2}{2\epsilon u_0 V_0} \tag{14.12}$$

$$P_e = \frac{A}{2\theta[K - (\theta_e - \theta)^2]} \tag{14.88}$$

Let us now expand (14.88) assuming K to be very small

$$P_e = \frac{A}{2\theta(\theta_e - \theta)^2} \left[1 + \frac{K}{(\theta_e - \theta)^2} + \cdots \right] \tag{14.89}$$

If we let

$$K = A/4 \tag{14.90}$$

we see that these first two terms agree with the expansion of the broad-beam expression, (14.77). The leading term was not adjusted; the space-charge parameter K was, since there is no other way of evaluating the parameter in this case.

In Fig. 14.9, the value of θP_e as obtained, actually, from (14.73) rather than (14.76), is plotted as a solid line and the value corresponding to the

earlier theory, from (14.86) with K adjusted according to (14.88), is plotted as a dashed line, for

$$A = 0.01$$

$$\theta_e = 8$$

We see that (14.88), which involves the approximations made in our earlier calculations concerning traveling-wave tubes, is a remarkably good fit to the broad-beam expression derived from field theory up very close to the points $(\theta_e - \theta) = A$, which are the boundaries between real and imaginary arguments of the hyperbolic tangent and correspond to the points where the ordinate is zero in Fig. 14.5.

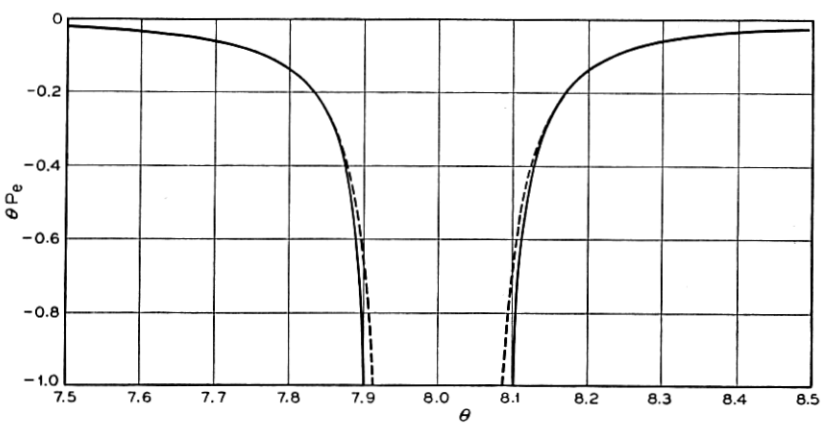

Fig. 14.9—These curves compare an exact electronic susceptance for the broad beam case (solid curve) with the approximate expression used earlier (dashed curve). In the approximate expression, the "effective current" was evaluated, not fitted; the space-charge parameter was chosen to give a fit.

Over the range in which the argument of the hyperbolic tangent in the correct expression is imaginary, the approximate expression of course exhibits none of the complex behavior characteristics of the correct expression and illustrated by Fig. 14.6. From (14.88) we see that the multiple excursions of the true curve from $-\infty$ to $+\infty$ are replaced in the approximate curve by a single dip down toward 0 and back up again. R. C. Fletcher has used a method similar to that explained above in computing the effective helix impedance and the effective space-charge parameter Q for a solid beam inside of a helically conducting sheet. His work, which is valuable in calculating the gain of traveling-wave tubes, is reproduced in Appendix VI.

14.5c *The Complex Roots*

The propagation constants represent intersections of a circuit curve such as that shown in Fig. 14.8 and an electronic curve such as that shown in Fig.

14.9. The propagation constants obtained in Chapters II and VIII represent such intersections of approximate circuit and electronic curves, such as the dotted lines of Fig. 14.8 and 14.9. Propagation constants obtained by field solutions represent intersections of the more nearly exact circuit and electronic curves such as the solid curves of Figs. 14.8 and 14.9.

If we plot a circuit curve giving

$$(1/\theta_0 \sqrt{\epsilon/\mu})(i/jE_z)$$

as given by (14.65) (the right-hand side of 14.75) and an electronic curve giving

$$(1/\theta_0 \sqrt{\epsilon/\mu})(i/jE_z) = P_e$$

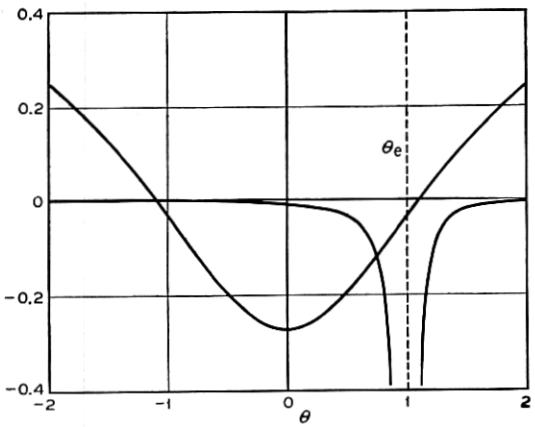

Fig. 14.10—The curves of Fig. 14.5 may be replaced by those of Fig. 14.6. Here the curve which is concave upward represents the circuit susceptance and the other curve represents the electronic susceptance (as in Fig. 14.9).

as given by (14.73) (the left-hand side of (14.72)), the plot, which is shown in Fig. 14.10, contains the same information as the plot of Fig. 14.5 for which θ_0, θ_e and A are the same. In Fig. 14.10, however, one curve represents the circuit without electrons and the other represents the added effect of the electrons.

We have seen that the approximate expressions of Chapter VII fit the broad-beam curves well for real propagation constants (real values of θ) (Fig. 14.8 and 14.9). Hence, we expect that complex roots corresponding to the increasing waves which are obtained using the approximate expressions will be quite accurate when the circuit curve is not too far from the electronic curve for real values of θ; that is, when the parameters (electron velocity, for instance) do not differ too much from those values for which the circuit curve is tangent to the electronic curve.

Unfortunately, the behavior of a function for values of the variables far

from those represented by its intersection with the real plane may be very sensitive to the shape of the intersection with the real plane. Thus, we would scarcely be justified by the good fit of the approximations represented in Figs. 14.8 and 14.9 in assuming that the complex roots obtained using the approximations will be good except when they correspond to a near approach of the electronic and circuit curves, as in Fig. 14.10.

In fact, using the approximate curves, we find that the increasing wave vanishes for electron velocities less than a certain lower limiting velocity. This corresponds to cutting by the circuit curve of the dip down from $+\infty$ of the approximate electronic curve (the dip is not shown in Fig. 14.9). This is not characteristic of the true solution. An analysis shows, however,

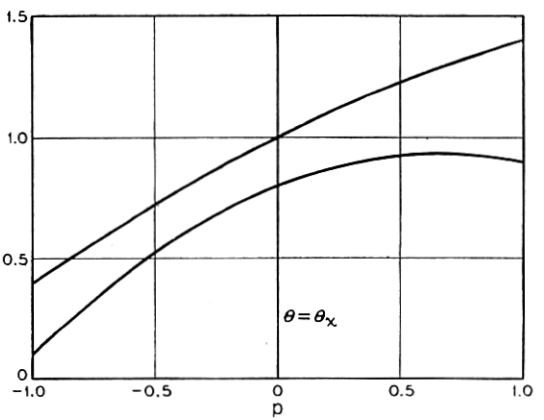

Fig. 14.11—Complex roots are obtained when curves such as those of Fig. 14.10 do not have the number of intersections required (by the degree of the equation) for real values of the abscissa and ordinate. In this figure, two parabolas narrowly miss intersect ng. Suppose these represent circuit and electronic susceptance curves. We find that the gain of the increasing wave will increase with the square root of the separation at the abscissa of equal slopes, and inversely as the square root of the difference in second derivatives.

that there will be a limiting electron velocity below which there is no increasing wave if there is a charge-free region between the electron flow and the circuit.

14.6 Some Remarks About Complex Roots

If we examine our generalized circuit expression (14.60) we see that the circuit impedance parameter $(E^2/\beta^2 P)$ is inversely proportional to the slope of the circuit curve at the point where it crosses the horizontal axis. Thus, low-impedance circuits cut the axis steeply and high-impedance circuits cut the axis at a small slope.

We cannot go directly from this information to an evaluation of gain in terms of impedance; the best course in this respect is to use the methods of

Chapter VIII. We can, however, show a relation between gain and the properties of the circuit and electronic curves for cases in which the curves almost touch (an electron velocity just a little lower than that for which gain appears). Suppose the curves nearly touch at $\theta = \theta_x$, as indicated in Fig. 14.11. Let

$$\theta = \theta_x + p \tag{14.91}$$

Let us represent the curves for small values of p by the first three terms of a Taylor's series. Let the ordinate y of the circuit curve be given by

$$y = a_1 + b_1 p + c_1 p^2 \tag{14.92}$$

and let the ordinate of the electronic curve be given by

$$y = a_2 + b_2 p + c_2 p^2 \tag{14.93}$$

Then, at the intersection

$$(c_1 - c_2)p^2 + (b_1 - b_2)p + (a_1 - a_2) = 0$$

$$p = -(1/2)\frac{b_1 - b_2}{c_1 - c_2} \pm j\sqrt{\frac{(a_1 - a_2)}{(c_1 - c_2)} - \frac{(b_1 - b_2)^2}{4(c_1 - c_2)^2}} \tag{14.94}$$

If we choose θ_x as the point at which the slopes are the same

$$b_1 - b_2 = 0 \tag{14.95}$$

$$p = \pm j\sqrt{\frac{(a_1 - a_2)}{(c_1 - c_2)}} \tag{14.96}$$

and we see that the imaginary part of p increases with the square root of the separation, and at a rate inversely proportional to the difference in second derivatives. This is exemplified by the behavior of x_1 and x_2 for b a little small than $(3/2)(2)^{1/3}$ in Fig. 8.1.

Now, referring to Fig. 14.10, we see that a circuit curve which cuts the axis at a shallow angle (a high-impedance circuit curve) will approach or be tangent to the electronic curve at a point where the second derivative is small, while a steep (low impedance) circuit curve will approach the electronic curve at a point where the second derivative is high. This fits in with the idea that a high impedance should give a high gain and a low impedance should give a low gain.

CHAPTER XV

MAGNETRON AMPLIFIER

Synopsis of Chapter

THE HIGH EFFICIENCY of the magnetron oscillator is attributed to motion of the electrons toward the anode (toward a region of higher d-c potential) at high r-f levels. Thus, an electron's loss of energy to the r-f field is made up, not by a slowing-down of its motion in the direction of wave propagation, but by abstraction of energy from the d-c field.[1]

Warnecke and Guenard[2] have published pictures of magnetron amplifiers and Brossart and Doehler have discussed the theory of such devices.[3]

No attempt will be made here to analyze the large-signal behavior of a magnetron amplifier or even to treat the small-signal theory extensively. However, as the device is very closely related to conventional traveling-wave tubes, it seems of some interest to illustrate its operation by a simple small-signal analysis.

The case analyzed is indicated in Fig. 15.1. A narrow beam of electrons flows in the $+z$ direction, constituting a current I_0. There is a magnetic field of strength B normal to the plane of the paper (in the x direction), and a d-c electric field in the y direction. The beam flows near to a circuit which propagates a slow wave. Fig. 15.3, which shows a finned structure opposed to a conducting plane and held positive with respect to it, gives an idea of a physical realization of such a device. The electron stream could come from a cathode held at some potential intermediate between that of the finned structure and that of the plane. In any event, in the analysis the electrons are assumed to have such an initial d-c velocity and direction as to make them travel in a straight line, the magnetic and electric forces just cancelling.

The circuit equation developed in Chapter XIII in connection with transverse motions of electrons is used. Together with an appropriate ballistical equation, this leads to a fifth degree equation for Γ.

[1] For an understanding of the high-level behavior of magnetrons the reader is referred to: J. B. Fisk, H. D. Hagstrum and P. L. Hartman, "The Magnetron as a Generator of Centimeter Waves," *Bell System Technical Journal*, Vol. XXV, April 1946.
"Microwave Magnetrons" edited by George B. Collins, McGraw-Hill, 1948.

[2] R. Warnecke and P. Guenard, "Sur L'Aide Que Peuvent Apporter en Television Quelques Recentes Conceptions Concernant Les Tubes Electroniques Pour Ultra-Hautes Frequences," *Annales de Radioelectricite*, Vol. III, pp. 259–280, October 1948.

[3] J. Brossart and O. Doehler, "Sur les Proprietes des Tubes a Champ Magnetique Constant: les Tubes a Propagation D'Onde a Champ Magnetique," *Annales de Radioelectricite*, Vol. III, pp. 328–338, October 1948.

The nature of this equation indicates that gain may be possible in two ranges of parameters. One is that in which the electron velocity is near to or equal to (as, (15.25)) the circuit phase velocity. In this case there is gain provided that the transverse component of a-c electric field is not zero, and provided that it is related to the longitudinal component as it is for the circuit of Fig. 15.3. It seems likely that this corresponds most nearly to usual magnetron operation.

The other interesting range of parameters is that near

$$\beta_e/\beta_1 = 1 - \beta_m/\beta_1 \tag{15.31}$$

Here β_e refers to the electrons, β_1 to the circuit and β_m is the cyclotron frequency divided by the electron velocity. When (15.31) holds, there is gain whenever the parameter α, which specifies the ratio of the transverse to the longitudinal fields, is not $+1$. For the circuit of Fig. 15.3, α approaccs $+1$ near the fins if the separation between the fins and the plane is great enough in terms of the wavelength. However, α can be made negative near the fins

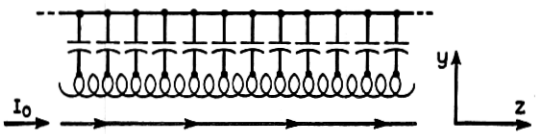

Fig. 15.1—In a magnetron amplifier a narrow electron stream travels in crossed electric and magnetic fields close to a wave transmission circuit.

if the potential of the fins is made negative compared with that of the plane, and the electrons are made to move in the opposite direction.

In either range of parameters, the gain of the increasing wave in db per wavelength is proportional to the square root of the current rather than to the cube root of the current. This means a lower gain than for an ordinary traveling-wave tube with the same circuit and current.

Increasing and decreasing waves with a negative phase velocity are possible when the magnetic field is great enough.

15.1 Circuit Equation

The circuit equation will be the same as that used in Chapter XIII, that is,

$$V = \frac{-j\omega\Gamma_1 K(\Phi\rho - (I_0/u_0)\Phi' y)}{(\Gamma^2 - \Gamma_1^2)} \tag{13.10}$$

It will be assumed that the voltage is given by

$$\Phi = (Ae^{-j\Gamma y} + Be^{j\Gamma y}) \tag{15.1}$$

so that

$$\Phi' V = -jV(Ae^{-j\Gamma y} - Be^{j\Gamma y}) \tag{15.2}$$

Atany$y$ — position we can write

$$\Phi' V = -j\Gamma\alpha\Phi V \tag{15.3}$$

$$\alpha = \frac{Ae^{-j\Gamma y} - Be^{j\Gamma y}}{Ae^{-j\Gamma y} + Be^{j\Gamma y}} \tag{15.4}$$

If Γ is purely imaginary, α is purely real, and as Γ will have only a small real component, α will be considered as a real number. We see that α can range from $+\infty$ to $-\infty$. For instance, consider a circuit consisting of opposed two-dimensional slotted members as shown in Fig. 15.2. For a field with a cosh distribution in the y direction, α is positive above the axis, zero on the axis and negative below the axis. For a field having a sinh distribution in the y

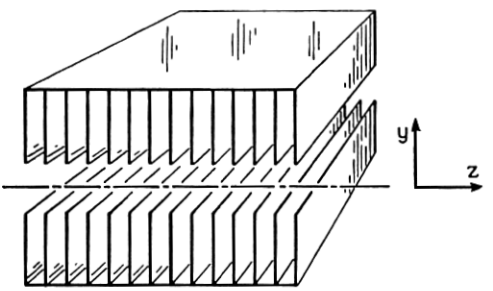

Fig. 15.2—If the circuit is as shown, the ratio between longitudinal and transverse field will be different in sign above and below the axis. This can have an important effect on th operation of the amplifier.

direction, α is infinite on the axis, positive above the axis and negative below the axis.

We find then, that, (13.10) becomes

$$V = \frac{-j\omega\Gamma_1\Phi K(\rho + j\alpha(I_0/u_0)\Gamma y)}{\Gamma^2 - \Gamma_1^2} \tag{15.5}$$

15.2 Ballistic Equations

The d-c electric field in the y direction will be taken as $-E_0$. Thus

$$\frac{d\dot{y}}{dt} = \eta\left[E_0 + \frac{\partial(\Phi V)}{\partial y} - B(z + u_0)\right] \tag{15.6}$$

In order to maintain a rectilinear unperturbed path

$$E_0 = Bu_0 \tag{15.7}$$

so that (15.6) becomes

$$\frac{d\dot{y}}{dt} = \eta\frac{\partial(\Phi V)}{\partial y} - \eta B^z \tag{15.8}$$

Following the usual procedure, we obtain

$$\dot{y} = \frac{-j\eta\Gamma\alpha\Phi V - \eta B^z}{u_0(j\beta_e - \Gamma)} \tag{15.9}$$

We have also

$$\frac{d\dot{z}}{dt} = \eta \frac{\partial \Phi V}{\partial x} + \eta B\dot{y}$$

$$\dot{z} = \frac{-\eta\Gamma\Phi V + \eta B\dot{y}}{u_0(j\beta_e - \Gamma)} \tag{15.10}$$

From (15.9) and (15.10) we obtain

$$z = \frac{-\eta\Gamma\Phi V[(j\beta_e - \Gamma) + j\alpha\beta_m]}{u_0[(j\beta_e - \Gamma)^2 + \beta_m^2]} \tag{15.11}$$

where

$$\beta_m = \omega_m/u_0 \tag{15.12}$$

$$\omega_m = \eta B \tag{15.13}$$

Here ω_m is the cyclotron radian frequency.

As before, we have

$$\rho = \frac{\Gamma\rho_0\dot{z}}{u_0(j\beta_e - \Gamma)} \tag{15.14}$$

whence

$$\rho = \frac{\Gamma^2\eta I_0\Phi V[(j\beta_e - \Gamma) + j\alpha\beta_m]}{u_0^3(j\beta_e - \Gamma)[(j\beta_e - \Gamma)^2 + \beta_m^2]} \tag{15.15}$$

We can also solve (15.9) and (15.10) for $\dot{y}$

$$\dot{y} = \frac{-j\eta\Gamma\Phi V[\alpha(j\beta_e - \Gamma) + j\beta_m]}{u_0[(j\beta_e - \Gamma)^2 + \beta_m^2]}. \tag{15.16}$$

Now, to the first order

$$\dot{y} = \frac{\partial y}{\partial t} + u_0 \frac{\partial y}{\partial z}$$

$$y = \frac{\dot{y}}{u_0(j\beta_e - \Gamma)} \tag{15.17}$$

and from (15.16) and (15.17)

$$y = \frac{-j\eta\Gamma\Phi V[\alpha(j\beta_e - \Gamma) + j\beta_m]}{u_0^2(j\beta_e - \Gamma)[(j\beta_e - \Gamma)^2 + \beta_m^2]}. \tag{15.18}$$

If we use (15.15) and (15.18) in connection with (15.5) we obtain

$$\Gamma^2 - \Gamma_1^2 = \frac{-j\beta_e \Gamma_1 \Gamma^2[(j\beta_e - \Gamma) + 2j[\alpha/(1+\alpha^2)]\beta_m]H^2}{(j\beta_e - \Gamma)[(j\beta_e - \Gamma)^2 + \beta_m^2]} \tag{15.19}$$

$$H^2 = \frac{(1+\alpha^2)\Phi^2 K I_0}{2V_0}. \tag{15.20}$$

Now let

$$-\Gamma_1 = -j\beta_1 \tag{15.21}$$

$$-\Gamma = -j\beta_1(1+p) \tag{15.22}$$

If we assume

$$p \ll 1 \tag{15.23}$$

and neglect p in sums in comparison with unity, we obtain

$$p(\beta_e/\beta_1 - 1 - p)[(\beta_e/\beta_1 - 1 - p)^2 - (\beta_m/\beta_1)^2] = -\frac{\beta_e}{2\beta_1}\left[(\beta_e/\beta_1 - 1 - p) + \frac{2\alpha\beta_m}{(1+\alpha^2)\beta_1}\right]H^2. \tag{15.24}$$

We are particularly interested in conditions which lead to an imaginary value of p which is as large as possible. We will obtain such large values of p when one of the factors multiplying p on the left-hand side of (15.24) is small. There are two possibilities. One is that the first factor is small. We explore this by assuming

$$\beta_e/\beta_1 - 1 = 0 \tag{15.25}$$

$$p^2\left(p^2 - \frac{\beta_m^2}{\beta_1^2}\right) = (1/2)\left(-p + \frac{2\alpha\beta_m}{(1+\alpha^2)\beta_1}\right)H^2, \tag{15.26}$$

If p is very small, we can write approximately

$$-p^2\frac{\beta_m^2}{\beta_1^2} = \frac{\alpha}{(1+\alpha^2)}\frac{\beta_m}{\beta_1}H^2$$
$$p = \pm j[\alpha/(1+\alpha^2)]^{1/2}(\beta_1/\beta_m)^{1/2}H \tag{15.27}$$

We see that p goes to zero if $\alpha = 0$ and is real if α is negative. If we consider what this means circuit-wise, we see that there will be gain with the d-c voltage applied between a circuit and a conducting plane as shown in Fig. 15.3.

Another possible condition in the neighborhood of which p is relatively large is

$$\beta_e/\beta_1 - 1 = \pm\,\beta_m/\beta_1 \tag{15.28}$$

In this case

$$p(\pm\beta_m/\beta_1 - p)(\mp 2(\beta_m/\beta_1)p + p^2) = -\left(1 \pm \frac{\beta_m}{\beta_1}\right)\left[(\pm\beta_m/\beta_1 - p) + \frac{2\alpha\beta_m}{(1+\alpha^2)\beta_1}\right]H^2. \tag{15.29}$$

As p is small, we write approximately

$$p^2 = \pm\frac{1}{4}\frac{(1 \pm \alpha)^2}{1+\alpha^2}\left(\frac{\beta_1}{\beta_m} \pm 1\right)H^2. \tag{15.30}$$

We see that we obtain an imaginary value of p only for the $-$ sign in (15.28) that is, if

$$\beta_e/\beta_1 = 1 - \beta_m/\beta_1 \tag{15.31}$$

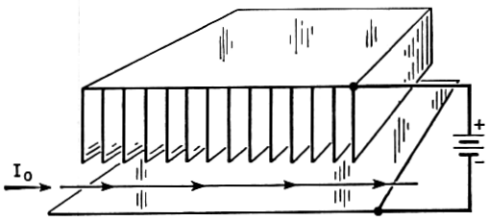

Fig. 15.3—The usual arrangement is to have the finned structure positive and opposed to a conducting plane.

In this case

$$p = \pm j\tfrac{1}{2}[(1-\alpha)/(1+\alpha)^{1/2}](\beta_e/\beta_m)^{1/2}H. \tag{15.32}$$

In this case we obtain gain for any value of α smaller than unity. We note that $\alpha = 1$ is the value α assumes far from the axis in a two-dimensional system of the sort illustrated in Fig. 15.2, for either a cosh or a sinh distribution in the $+y$ direction.

The assumption of $-\Gamma = -j\beta_1(1+p)$ in (15.22) will give forward ($+z$) traveling-waves only. In order to investigate backward traveling-waves, we must assume

$$-\Gamma = +j\beta_1(1+p) \tag{15.33}$$

where again p is considered a small number. If we use this in (15.19), we obtain

$$p\left(\frac{\beta_e}{\beta_1} + 1 + p\right)\left[\left(\frac{\beta_e}{\beta_1} + 1 + p\right)^2 - \frac{\beta_m^2}{\beta_1^2}\right] = -\frac{1}{2}\frac{\beta_e}{\beta_1}\left[\left(\frac{\beta_e}{\beta_1} + 1 + p\right) + \frac{2\alpha\beta_m}{(1+\alpha^2)\beta_1}\right]H^2. \tag{15.34}$$

As before we look for solutions for p where the terms multiplying p on the left are small. The only vanishing consistent with positive values of β_e and β_1 is obtained for

$$\frac{\beta_e}{\beta_1} + 1 = +\frac{\beta_m}{\beta_1}. \tag{15.35}$$

Under this condition (15.34) yields for p

$$p = \pm j \frac{1}{2} \frac{(1 + \alpha)}{(1 + \alpha^2)^{1/2}} \left(\frac{\beta_e}{\beta_m}\right)^{1/2} H. \tag{15.36}$$

Thus we can obtain backward-increasing backward-traveling waves for all values of α except $\alpha = -1$. For the situation shown in Fig. 15.3, with a backward wave, α is always negative, approaching -1 at large distances from the plane electrode, so that the gain is identical with that given by (15.32).

We note that (15.27), (15.32) and (15.36) show that p is proportional to the product of current times impedance divided by voltage to the $\frac{1}{2}$ power, while, in the case of the usual traveling-wave tube, this small quantity occurs to the $\frac{1}{3}$ power. The $\frac{1}{3}$ power of a small quantity is larger than the $\frac{1}{2}$ power; and, hence for a given circuit impedance, current and voltage, the gain of the magnetron amplifier will be somewhat less than the gain of a conventional traveling-wave tube.

CHAPTER XVI

DOUBLE-STREAM AMPLIFIERS

Synopsis of Chapter

IN TRAVELING-WAVE TUBES, it is desirable to have the electrons flow very close to the metal circuit elements, where the radio-frequency field of the circuit is strong, in order to obtain satisfactory amplification. It is, however, difficult to confine the electron flow close to metal circuit elements without an interception of electrons, which entails both loss of efficiency and heating of the circuit elements. This latter may be extremely objectionable at very short wavelengths for which circuit elements are small and fragile.

In the double-stream amplifier the gain is not obtained through the interaction of electrons with the field of electromagnetic resonators, helices or other circuits. Instead, an electron flow consisting of two streams of electrons having different average velocities is used. When the currents or charge densities of the two streams are sufficient, the streams interact so as to give an increasing wave.[1,2,3,4] Electromagnetic circuits may be used to impress a signal on the electron flow, or to produce an electromagnetic output by means of the amplified signal present in the electron flow. The amplification, however, takes place in the electron flow itself, and is the result of what may be termed an electromechanical interaction.[5]

While small magnetic fields are necessarily present because of the motions of the electrons, these do not play an important part in the amplification. The important factors in the interaction are the electric field, which stores energy and acts on the electrons, and the electrons themselves. The charge of the electrons produces the electric field; the mass of the electrons, and their kinetic energy, serve much as do inductance and magnetic stored energy in electromagnetic propagation.

[1] J. R. Pierce and W. B. Hebenstreit, "A New Type of High-Frequency Amplifier," *B.S.T.J.*, Vol. 28, pp. 33–51, January 1949.

[2] A. V. Hollenberg, "Experimental Observation of Amplification by Interaction between Two Electron Streams," *B.S.T.J.*, Vol. 28, pp. 52–58, January 1949.

[3] A. V. Haeff, "The Electron-Wave Tube—A Novel Method of Generation and Amplification of Microwave Energy," *Proc. IRE*, Vol. 37, pp. 4–10, January 1949.

[4] L. S. Nergaard, "Analysis of a Simple Model of a Two-Beam Growing-Wave Tube," *R.C.A. Review*, Vol. 9, pp. 585–601, December 1948.

[5] Some similar electromechanical waves are described in papers by J. R. Pierce, "Possible Fluctuations in Electron Streams Due to Ions," *Jour. App. Phys.*, Vol. 19, pp. 231–236, March 1948, and "Increasing Space-Charge Waves," *Jour. App. Phys.*, Vol. 20 pp. 1060–1066, Nov. 1949.

By this sort of interaction, a traveling wave which increases as it travels, i.e., a traveling wave of negative attenuation, may be produced. To start such a wave, the electron flow may be made to pass through a resonator or a short length of helix excited by the input signal. Once initiated, the wave grows exponentially in amplitude until the electron flow is terminated or until non-linearities limit the amplitude. An amplified output can be obtained by allowing the electron flow to act on a resonantor, helix or other output circuit at a point far enough removed from the input circuit to give the desired gain.

In general, for a given geometry there is a limiting value of current below which there is no increasing wave. For completely intermingled electron streams, the gain rises toward an asymptotic limit as the current is increased beyond this value. The ordinate of Fig. 16.3 is proportional to gain and the abscissa to current.

When the electron streams are separated, the gain first rises and then falls as the current is increased. This effect, and also the magnitude of the increasing wave set up by velocity modulating the electron streams, have been discussed in the literature.[6]

Double-stream amplifiers have several advantages. Because the electrons interact with one another, the electron flow need not pass extremely close to complicated circuit elements. This is particularly advantageous at very short wavelengths. Further, if we make the distance of electron flow between the input and output circuits long enough, amplification can be obtained even though the input and output circuits have very low impedance or poor coupling to the electron flow. Even though the region of amplification is long, there is no need to maintain a close synchronism between an electron velocity and a circuit wave velocity, as there is in the usual traveling-wave tube.

16.1 Simple Theory of Double-Stream Amplifiers

For simplicity we will assume that the flow consists of coincident streams of electrons of d-c velocities u_1 and u_2 in the z direction. It will be assumed that there is no electron motion normal to the z direction. M.K.S. units will be used.

It turns out to be convenient to express variation in the z direction as

$$\exp -j\beta z$$

rather than as

$$\exp -\Gamma z$$

[6] J. R. Pierce, "Double-Stream Amplifiers," *Proc. I.R.E.*, Vol. 37, pp. 980–985, Sept. 1949.

as we have done previously. This merely means letting

$$\Gamma = j\beta \tag{16.1}$$

The following nomenclature will be used

J_1 , J_2 d-c current densities
u_1 , u_2 d-c velocities
ρ_{01} , ρ_{02} d-c charge densities

$$\rho_{01} = -J_1/u_1 \text{ , } \rho_{02} = -J_2/u_2$$

ρ_1 , ρ_2 a-c charge densities
v_1 , v_2 a-c velocities
V_1 , V_2 d-c voltages with respect to the cathodes
V a-c potential
$\beta_1 = \omega/u_1$, $\beta_2 = \omega/u_2$

From (2.22) and (2.18) we obtain

$$\rho_1 = \frac{\eta J_1 \beta^2 V}{u_1^3(\beta_1 - \beta)^2} \tag{16.2}$$

and

$$\rho_2 = \frac{\eta J_2 \beta^2 V}{u_2^3(\beta_2 - \beta)^2}. \tag{16.3}$$

It will be convenient to call the fractional velocity separation b, so that

$$b = \frac{2(u_1 - u_2)}{u_1 + u_2}. \tag{16.4}$$

It will also be convenient to define a sort of mean velocity u_0

$$u_0 = \frac{2u_1 u_2}{u_1 + u_2}. \tag{16.5}$$

We may also let V_0 be the potential drop specifying a velocity u_0 , so that

$$u_0 = \sqrt{2\eta V_0} \tag{16.6}$$

It is further convenient to define a phase constant based on u_0

$$\beta_e = \frac{\omega}{u_0}. \tag{16.7}$$

We see from (16.4), (16.5) and (16.6) that

$$\beta_1 = \beta_e(1 - b/2) \tag{16.8}$$

$$\beta_2 = \beta_e(1 + b/2) \tag{16.9}$$

We shall treat only a special case, that in which

$$\frac{J_1}{u_1^3} = \frac{J_2}{u_2^3} = \frac{J_0}{u_0^3}. \tag{16.10}$$

Here J_0 is a sort of mean current which, together with u_0, specifies the ratios J_1/u_1^3 and J_2/u_2^3, which appear in (4) and (5).

In terms of these new quantities, the expression for the total a-c charge density ρ is, from (16.2) and (16.3) and (16.6)

$$\rho = \rho_1 + \rho_2 = \frac{J_0\beta^2}{2u_0 V_0} \cdot \left[\frac{1}{\left[\beta_e\left(1 - \frac{b}{2}\right) - \beta\right]^2} + \frac{1}{\left[\beta_e\left(1 + \frac{b}{2}\right) - \beta\right]^2}\right] V. \tag{16.11}$$

Equation (16.11) is a *ballistic* equation telling what charge density ρ is produced when the flow is bunched by a voltage V. To solve our problem, that is, to solve for the phase constant β, we must associate (16.11) with a *circuit* equation which tells us what voltage V the charge density produces. We assume that the electron flow takes place in a tube too narrow to propagate a wave of the frequency considered. Further, we assume that the wave velocity is much smaller than the velocity of light. Under these circumstances the circuit problem is essentially an electrostatic problem. The a-c voltage will be of the same sign as, and in phase with the a-c charge density ρ. In other words the "circuit effect" is purely capacitive.

Let us assume at first that the electron stream is very narrow compared with the tube through which it flows, so that V may be assumed to be constant over its cross section. We can easily obtain the relation between V and ρ in two extreme cases. If the wavelength in the stream is very short (β large), so that transverse a-c fields are negligible, then, from Poisson's equation, we have

$$\rho = -\epsilon \frac{\partial^2 V}{\partial z^2}$$
$$\rho = \epsilon\beta^2 V \tag{16.12}$$

If, on the other hand, the wavelength is long compared with the tube radius (β small) so that the fields are chiefly transverse, the lines of force running from the beam outward to the surrounding tube, we may write

$$\rho = CV \tag{16.13}$$

Here C is a constant expressing the capacitance per unit length between the region occupied by the electron flow and the tube wall.

We see from (16.12) and (16.13) that, if we plot ρ/V vs. β/β_e for real values of β, ρ/V will be constant for small values of β and will rise as β^2 for large values of β, approximately as shown in Fig. 16.1.

Now, we have assumed that the charge is produced by the action of the voltage, according to the ballistical equation (16.11). This relation is plotted in Fig. 2, for a relatively large value of J_0/u_0V_0 (curve 1) and for a smaller value of J_0/u_0V_0 (curve 2). There are poles at $\beta/\beta_e = 1 \pm \frac{b}{2}$, and a minimum between the poles. The height of the minimum increases as J_0/u_0V_0 is increased.

A circuit curve similar to that of Fig. 16.1 is also plotted on Fig. 16.2. We see that for the small-current case (curve 2) there are four intersections, giving *four real* values of β and hence *four unattenuated* waves. However, for

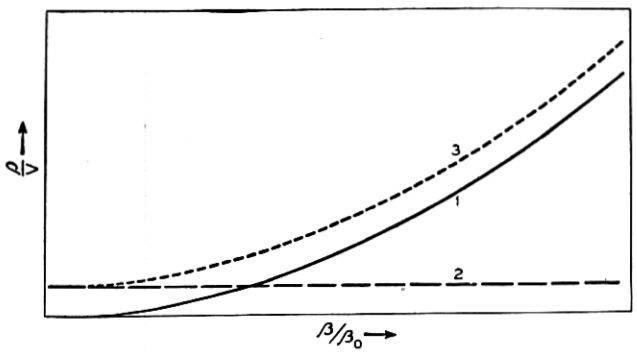

Fig. 16.1—Circuit curves, in which the ordinate is proportional to the ratio of the charge per unit length to the voltage which it produces. Curve 1 is for an infinitely broad beam; curve 2 is for a narrow beam in a narrow tube. Curve 3 is the sum of 1 and 2, and approximates an actual curve.

the larger current (curve 1) there are only two intersections and hence two unattenuated waves. The two additional values of β satisfying both the circuit equation and the ballistical equation are complex conjugates, and represent waves traveling at the same speed, but with equal positive negative attenuations.

Thus we deduce that, as the current densities in the electron streams are raised, a wave with negative attenuation appears for current densities above a certain critical value.

We can learn a little more about these waves by assuming an approximate expression for the circuit curve of Fig. 1. Let us merely assume that over the range of interest (near $\beta/\beta_e = 1$) we can use

$$\rho = \alpha^2\epsilon\beta^2 V \tag{16.14}$$

Here α^2 is a factor greater than unity, which merely expresses the fact that the charge density corresponding to a given voltage is somewhat greater than if there were field in the z direction only for which equation (16.12) is valid. Combining (16.14) with (16.11) we obtain

$$\frac{1}{\left(\beta_e\left(1-\frac{b}{2}\right)-\beta\right)^2}+\frac{1}{\left(\beta_e\left(1+\frac{b}{2}\right)-\beta\right)^2}=\frac{1}{\beta_e^2 U^2} \tag{16.15}$$

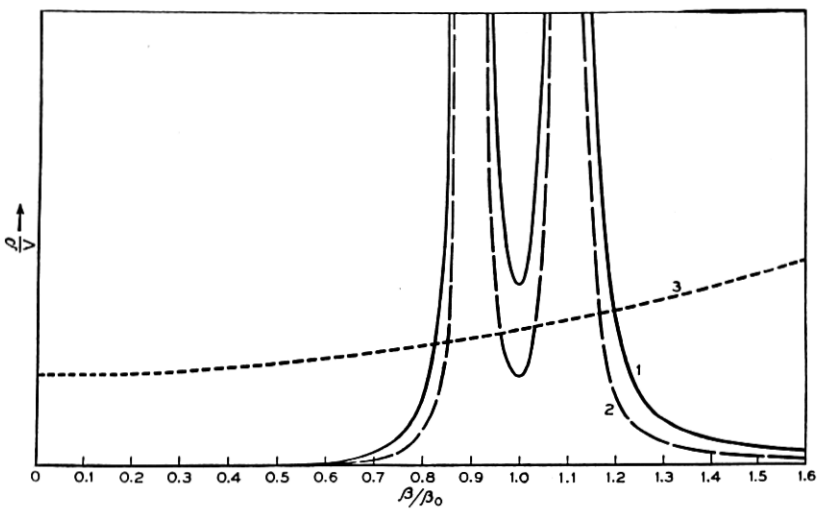

Fig. 16.2—This shows a circuit curve, 3, and two electronic curves which give the sum of the charge densities of the two streams divided by the voltage which bunches them. With curve 2, there will be four unattenuated waves. With curve 1, which is for a higher current density than curve 2, there are two unattenuated waves, an increasing wave and a decreasing wave.

where

$$U^2=\frac{J_0}{2\alpha^2\epsilon\beta_e^2 u_0 V_0}. \tag{16.16}$$

In solving (16.15) it is most convenient to represent β in terms of β_e and a new variable h

$$\beta=\beta_e(1+h) \tag{16.17}$$

Thus, (16.15) becomes

$$\frac{1}{\left(h-\frac{b}{2}\right)^2}+\frac{1}{\left(h+\frac{b}{2}\right)^2}=\frac{1}{U^2}. \tag{16.18}$$

Solving for h, we obtain

$$h = \pm\left(\frac{b}{2}\right)\left[\left(\frac{2U}{b}\right)^2 + 1 \pm \left(\frac{2U}{b}\right)\sqrt{\left(\frac{2U}{b}\right)^2 + 4}\right]^{1/2}. \quad (16.19)$$

The positive sign inside of the brackets always gives a real value of h and hence unattenuated waves. The negative sign inside the brackets gives unattenuated waves for small values of U/b. However, when

$$\left(\frac{U}{b}\right)^2 > \frac{1}{8} \quad (16.20)$$

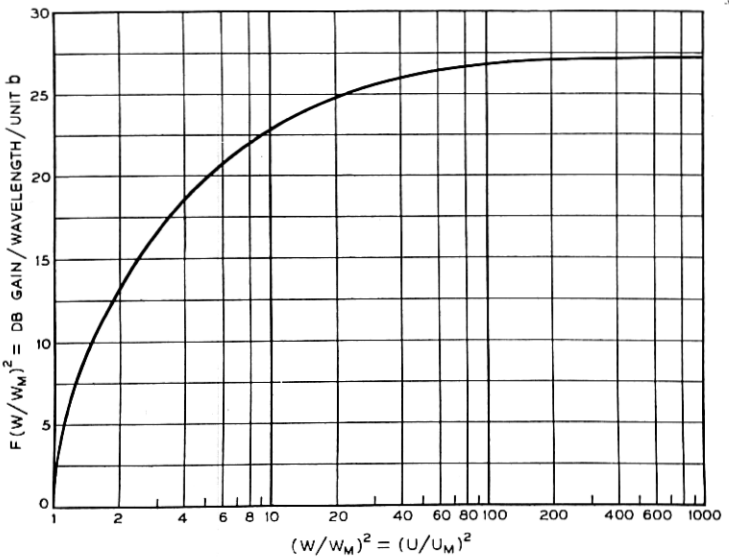

Fig. 16.3—The abscissa is proportional to d-c current. As the current is increased, the gain in db per wavelength approaches 27.3b, where b is the fractional separation in velocity. If the two electron streams are separated physically, the gain is lower and first rises and then falls as the current is increased.

there are two waves with a phase constant β_e and with equal and opposite attenuation constants.

Suppose we let U_M be the minimum value of U for which there is gain. From (16.20)

$$U_M^2 = b^2/8 \quad (16.21)$$

From (16.19) we have, for the increasing wave,

$$h = jb\left[\frac{U}{\sqrt{2}\,U_M}\sqrt{2\left(\frac{U}{U_M}\right)^2 + 1} - \left(\frac{U}{U_M}\right)^2 - 1\right]^{1/2}. \quad (16.22)$$

The gain in db/wavelength is

$$\text{db/wavelength} = 20(2\pi)\log_{10}e^{|h|}$$
$$= 54.6\,|\,h\,| \qquad (16.23)$$

We see that, by means of (16.22) and (16.23), we can plot db/wavelength per unit b vs. $(U/U_M)^2$. This is plotted in Fig. 16.3. Because U^2 is proportional to current, the variable $(U/U_M)^2$ is the ratio of the actual current to the current which will just give an increasing wave. If we know this ratio, we can obtain the gain in db/wavelength by multiplying the corresponding ordinate from Fig. 16.3 by b.

We see that, as the current is increased, the gain per wavelength at first rises rapidly and then rises more slowly, approaching a value $27.3b$ db/wavelength for very large values of $(U/U_M)^2$.

We now have some idea of the variation of gain per wavelength with velocity separation b and with current $(U/U_M)^2$. A more complete theory requires the evaluation of the lower limiting current for gain (or of U_M^2) in terms of physical dimensions and an investigation of the boundary conditions to show how strong an increasing wave is set up by a given input signal.[1, 6]

16.2 Further Considerations

There are a number of points to be brought out concerning double-stream amplifiers. Analysis shows[6] that any physical separation of the electron streams has a very serious effect in reducing gain. Thus, it is desirable to intermingle the streams thoroughly if possible.

If the electron streams have a fractional velocity spread due to space charge which is comparable with the deliberately imposed spread b, we may expect a reduction in gain.

Haeff[3] describes a single-stream tube and attributes its gain to the space-charge spread in velocities. In his analysis of this tube he divides the beam into a high and a low velocity portion, and assigns the mean velocity to each. This is not a valid approximation.

Analysis indicates that a multiply-peaked distribution of current with velocity is necessary for the existent increasing waves, and gain in a "single stream" of electrons is still something of a mystery.

CHAPTER XVII

CONCLUSION

ALTHOUGH THIS BOOK contains some descriptive material concerning high-level behavior, it is primarily a treatment of the linearized or low-level behavior of traveling-wave tubes and of some related devices. In the case of traveling-wave tubes with longitudinal motion of electrons only, the treatment is fairly extended. In the discussions of transverse fields, magnetron amplifiers and double-stream amplifiers, it amounts to little more than an introduction.

One problem to which the material presented lends itself is the calculation of gain of longitudinal-field traveling-wave tubes. To this end, a summary of gain calculation is included as Appendix VII.

Further design information can be worked out as, for instance, exact gain curves at low gain with lumped or distributed loss, perhaps taking the space-charge parameter QC into account, or, a more extended analysis concerning noise figure.

The material in the book may be regarded from another point of view as an introduction, through the treatment of what are really very simple cases, to the high-frequency electronics of electron streams. That is, the reader may use the book merely to learn how to tackle new problems. There are many of these.

One serious problem is that of extending the non-linear theory of the traveling-wave tube. For one thing, it would be desirable to include the effects of loss and space charge. Certainly, a matter worthy of careful investigation is the possibility of increasing efficiency by the use of a circuit in which the phase velocity decreases near the output end. Nordsieck's work can be a guide in such endeavors.

Even linear theory excluding the effects of thermal velocities could profitably be extended, especially to disclose the comparative behavior of narrow electron beams and of broad beams, both those confined by a magnetic field, in which transverse d-c velocities are negligible and in which space charge causes a lowering of axial velocity toward the center of the beam, and also those in which transverse a-c velocities are allowed, especially the Brillouin-type flow, in which the d-c axial velocity is constant across the beam, but electrons have an angular velocity proportional to radius.

Further problems include the extension of the theory of magnetron amplifiers and of double-stream amplifiers to a scope comparable with that of the

theory of conventional traveling-wave tubes. The question of velocity distribution across the beam is particularly important in double-stream amplifiers, whose very operation depends on such a distribution, and it is important that the properties of various kinds of distribution be investigated.

Finally, there is no reason to suspect that the simple tubes described do not have undiscovered relatives of considerable value. Perhaps diligent work will uncover them.

BIBLIOGRAPHY

1946

Barton, M. A. Traveling wave tubes, *Radio*, v. 30, pp. 11–13, 30–32, Aug., 1946.

Blanc-Lapierre, A. and Lapostolle, P. Contribution à l'étude des amplificateurs à ondes progressives, *Ann. des Telecomm.*, v. 1, pp. 283–302, Dec., 1946.

Kompfner, R. Traveling wave valve—new amplifier for centimetric wavelengths. *Wireless World*, v. 52, pp. 369–372, Nov., 1946.

Pierce, J. R. Beam traveling-wave tube, *Bell Lab. Record*, v. 24, pp. 439–442, Dec., 1946.

1947

Bernier, J. Essai de théorie du tube électronique à propagation d'onde, *Ann. de Radioélec.*, v. 2, pp. 87–101, Jan., 1947. *Onde Élec.*, v. 27, pp. 231–243, June, 1947.

Blanc-Lapierre, A., Lapostolle, P., Voge, J. P., and Wallauschek, R. Sur la théorie des amplificateurs à ondes progressives, *Onde Élec.*, v. 27, pp. 194–202, May, 1947.

Kompfner, R. Traveling-wave tuge as amplifier at microwaves, *I.R.E., Proc.*, v. 35, pp. 124–127, Feb., 1947.

Kompfner, R. Traveling-wave tube—centimetre-wave amplifier, *Wireless Engr.*, v. 24, pp. 255–266, Sept., 1947.

Pierce, J. R. Theory of the beam-type traveling-wave tube, *I.R.E., Proc.*, v. 35, pp. 111–123, Feb., 1947.

Pierce, J. R. and Field, L. M. Traveling-wave tubes, *I.R.E., Proc.*, v. 35, pp. 108–111, Feb., 1947.

Roubine, E. Sur le circuit à hélice utilisé dans le tube à ondes progressives, *Onde Élec.*, v. 27, pp. 203–208, May, 1947.

Shulman, C. and Heagy, M. S. Small-signal analysis of traveling-wave tube, *R.C.A. Rev.*, v. 8, pp. 585–611, Dec., 1947.

1948

Brillouin, L. Wave and electrons traveling together—a comparison between traveling wave tubes and linear accelerators, *Phys. Rev.*, v. 74, pp. 90–92, July 1, 1948.

Brossart, J. and Doehler, O. Sur les propriétés des tubes à champ magnétique constant. Les tubes à propagation d'onde à champ magnétique, *Ann. de Radioélec.*, v. 3, pp. 328–338, Oct., 1948.

Cutler, C. C. Experimental determination of helical-wave properties, *I.R.E., Proc.*, v. 36, pp. 230–233, Feb., 1948.

Chu, L. J. and Jackson, J. D. Field theory of traveling-wave tubes, *I.R.E., Proc.*, v. 36, pp. 853–863, July, 1948.

Döehler, O. and Kleen, W. Phénomènes non lineaires dans les tubes à propagation d'onde. *Ann. de Radioélec.*, v. 3, pp. 124–143, Apr., 1948.

Döehler, O. and Kleen, W. Sur l'influence de la charge d'espace dans le tube à propagation d'onde, *Ann. de Radioélec.*, v. 3, pp. 184–188, July, 1948.

Blanc-Lapierre, A., Kuhner, M., Lapostolle, P., Jessel, M. and Wallauschek, R. Étude et réalisation d'amplificateurs à hélice. *Ann. des Telecomm.*, v. 3, pp. 257–308, Aug.–Sept., 1948.

Blanc-Lapierre, A. and Kuhner, M. Réalisation d'amplificateurs à onde progressive à hélice. Résultats généraux, pp. 259–264.

Lapostolle, P. Les phénomènes d'interaction dans le tube à onde progressive, Théorie et vérifications expérimentales, pp. 265–291.

Jessel, M. and Wallauschek, R. Étude expérimentale de la propagation de long d'une ligne à retard en forme d'hélice, pp. 291–299.

Wallauschek, R. Détérmination expérimentale des caractéristiques d'amplificateurs à onde progressive, Résultats obtenus, pp. 300–308.

Lapostolle, P. Étude des diverses ondes susceptibles de se propager dans une ligne en interaction avec un faisceau électronique. Application à la théorie de l'amplificateur à onde progressive, *Ann. des Telecomm.*, v. 3, pp. 57–71, Feb., pp. 85–104, Mar., 1948.

Pierce, J. R. Effect of passive modes in traveling wave tubes, *I.R.E., Proc.*, v. 36, pp. 993–997, Aug., 1948.
Pierce, J. R. Transverse fields in traveling-wave tubes, *Bell Sys. Tech. Jl.*, v. 27, pp. 732–746, Oct., 1948.
Rydbeck, O. E. H. Theory of the traveling-wave tube, *Ericsson Technics*, no. 46, pp. 3–18, 1948.
Tomner, J. S. A. Experimental development of traveling-wave tubes, Acta Polytech., *Elec. Engg.*, v. 1, no. 6, pp. 1–21, 1948.
Nergaard, L. S. Analysis of a simple model of a two-beam growing-wave tube, RCA Rev. vol. 9, pp. 585–601, Dec. 1948.

1949

Doehler, O. and Kleen, W. Influence du vecteur électrique transversal dans la ligne à retard du tube à propagation d'onde, *Ann. de Radioélec.*, v. 4, pp. 76–84, Jan., 1949.
Bruck, L. Comparison des valeurs mesurees pour le gain lineaine du tube à propagation d'onde avec les valeurs indiquées par diverses theories. *Annales de Radioélectricete*, v. IV, pp. 222–232, July, 1949.
Döehler, O. and Kleen, W. Sur le rendement du tube à propagation d'onde. *Annales de Radioélectricete*, v. IV, pp. 216–221, July, 1949.
Döehler, O., Kleen, W. and Palluel, P. Les tubes à propagation d'onde comme oscillateurs à large bande d'accord électronique. *Ann. de Radioélec.*, v. 4, pp. 68–75, Jan., 1949.
Döhler, O. and Kleen, W. Über die Wirkungsweise der "Traveling-Wave" Röhre. *Arch. Elektr. Übertragung*, v. 3, pp. 54–63, Feb., 1949.
Field, L. M. Some slow-wave structures for traveling-wave tubes. *I.R.E., Proc.*, v. 37, pp. 34–40, Jan., 1949.
Guenard, P., Berterattiere, R. and Doehler, O. Amplification par interaction electronque dans des tubes sans circuits. *Annales de Radioélectricete*, v. IV, pp. 171–177, July, 1949.
Laplume, J. Théorie du tube à onde progressive. *Onde Élec.*, v. 29, pp. 66–72, Feb., 1949.
Loshakov, L. N. On the propagation of Waves along a coaxial spiral line in the presence of an electron beam. *Zh. Tech. Fiz.*, vol. 19, pp. 578–595, May, 1949.
Dewey, G. C. A periodic-waveguide traveling-wave amplifier for medium powers. *Proc. N.E.C.* (Chicago), v. 4, p. 253, 1948.
Pierce, J. R. and Hebenstreit, W. B. A new type of high-frequency amplifier, Bell System Technical Journal, v. 28, pp. 33–51, January, 1949.
Haeff, A. V. The electron-wave tube—a novel method of generation and amplification of microwave energy. *Proc. I.R.E.*, v. 37, pp. 4–10, January, 1949.
Hollenberg, A. V. The double-stream amplifier, *Bell Laboratories Record*, v. 27, pp. 290–292, August, 1949.
Guenard, P., Berterottiere, R. and Döehler, O. Amplification by direct electronic interaction in valves without circuits, *Ann. Radioelec.*, v. 4, pp. 171–177, July, 1949.
Rogers, D. C. Traveling-wave amplifier for 6 to 8 centimeters, *Elec. Commun.* (London), v. 26, pp. 144–152, June, 1949.
Field, L. M. Some slow wave structures for traveling-wave tubes, *Proc. I.R.E.*, v. 37, pp. 34–40, January, 1949.
Schnitzer, R. and Weber, D. *Frequenz*, v. 3, pp. 189–196, July, 1949.
Pierce, J. R. Circuits for traveling-wave tubes, *Proc. I.R.E.*, v. 37, pp. 510–515, May, 1949.
Pierce, J. R. and Wax, N. A note on filter-type traveling-wave amplifiers, *Proc. I.R.E.*, v. 37, pp. 622–625, June, 1949.